

---

# COLLABORATIVE OPTIMIZATION OF MULTICLASS IMBALANCED LEARNING: DENSITY-AWARE AND REGION-GUIDED BOOSTING

---

A PREPRINT

Chuantao Li<sup>†1,2</sup>, Zhi Li<sup>†1</sup>, Jiahao Xu<sup>1</sup>, Jie Li<sup>1</sup>, and Sheng Li<sup>\*1</sup>

<sup>1</sup>School of Mathematics and Computer, Guangdong Ocean University, Zhanjiang 524088, China

<sup>2</sup>School of Automation Engineering, University of Electronic Science and Technology of China, Chengdu, 611731, Sichuan, China

December 30, 2025

## ABSTRACT

Numerous studies attempt to mitigate classification bias caused by class imbalance. However, existing studies have yet to explore the collaborative optimization of imbalanced learning and model training. This constraint hinders further performance improvements. To bridge this gap, this study proposes a collaborative optimization Boosting model of multiclass imbalanced learning. This model is simple but effective by integrating the density factor and the confidence factor, this study designs a noise-resistant weight update mechanism and a dynamic sampling strategy. Rather than functioning as independent components, these modules are tightly integrated to orchestrate weight updates, sample region partitioning, and region-guided sampling. Thus, this study achieves the collaborative optimization of imbalanced learning and model training. Extensive experiments on 20 public imbalanced datasets demonstrate that the proposed model significantly outperforms eight state-of-the-art baselines. The code for the proposed model is available at: <https://github.com/Chuantaoli/DARG>.

**Keywords** Imbalanced Learning · Collaborative Optimization · Ensemble Learning · Sample Weight Update

## 1 Introduction

In industrial applications such as fault classification [1], medical diagnosis [2], network intrusion detection [3], and image recognition [4], data often exhibits a pronounced long-tail distribution. This class imbalance poses a fundamental challenge in machine learning. Minority class samples contribute negligibly to the aggregate training loss, resulting in models that favor the majority class. Consequently, the learner often fails to capture discriminative patterns from minority samples. While a model might achieve high overall accuracy, this metric is often misleading and of limited practical use, as the majority class dominates the predictions.

Researchers have developed numerous imbalanced learning methodologies over the past two decades, generally categorized into data-level and algorithm-level [5, 6]. Data-level methodologies use resampling to rebalance the sample distribution, enhancing the model’s ability to learn from minority classes. However, by artificially sampling or removing samples, these methods risk causing overfitting, information loss, or class overlap [7–9]. To improve the sampling quality, region-based strategies have become the prevalent paradigm. Unlike traditional methods like SMOTE [7] and ADASYN [10] that synthesize samples directly, recent studies prioritize initial data clustering followed by intra-cluster sampling. This ensures that generated samples more faithfully obey the original distribution [11–13].

In contrast, algorithm-level methodologies modify loss functions or misclassification costs to prioritize minority samples [14, 15]. However, effectively configuring cost matrices or sample weights remains difficult. Furthermore, these weights

---

<sup>\*</sup> Corresponding author.

<sup>†</sup>These authors contributed equally to this work.

*E-mail addresses:* 11672411dd@stu.gdou.edu.cn (C. Li), lizhi@gdou.edu.cn (Z. Li), xujh284@stu.gdou.edu.cn (J. Xu), lj@stu.gdou.edu.cn (J. Li), lish\_ls@gdou.edu.cn (S. Li)

typically stay static during training, making it nearly impossible to optimize them collaboratively with the model. To address this, some researchers embed sampling modules into the Boosting process. By modifying the training distribution before each iteration, the base learner can treat the minority class more equitably, while the classification error rate of each base learner is calculated to update the sample weights [16–18].

Despite these advancements, inherent limitations still persist. In many datasets, no distinct decision boundaries exist between majority and minority classes. For data-level methodologies, isolated noise samples often degrade the quality of region partitioning and sample generation, blurring decision boundaries and inducing class overlap. For algorithm-level methodologies, most existing studies merely splice the sampling module into the Boosting process rather than achieving deep coupling. Additionally, most methods target binary classification and do not extend to multiclass scenarios.

We observe that the AdaBoost weight update mechanism provides a bridge to collaboratively optimize the sampling module and the Boosting process. Crucially, this synergy allows us to integrate the complementary perspectives of both methodologies: whereas data-level methodologies use neighbors or distances to quantify sample density and region information, algorithm-level methodologies use prediction probabilities and training states to evaluate sample difficulty. By incorporating density and confidence information into the weight update mechanism, it can guide the base learner to focus on high-value samples while mitigating noise interference. This approach remedies a key deficiency in traditional AdaBoost, which focuses indiscriminately on all misclassified samples at each epoch. Furthermore, sampling module does not only provide a balanced distribution but also executes dynamic sampling tailored to each base learner and sample region based on the current training state.

Moving beyond a single research path, we focus on the cooperative optimization of imbalanced learning and model training. This study proposes Density-Aware and Region-Guided Boosting for multiclass imbalance. Our main contributions are:

- (1) **A noise-resistant sample weight update mechanism based on dual factors.** By devising a density factor based on mutual nearest neighbors and a confidence factor based on classification hardness, the proposed mechanism distinguishes between noise and genuinely hard samples, assigning higher weights to high-value samples.
- (2) **A cooperative optimization model for sample region partitioning and weight updates.** Based on density factor and confidence factor, this study partitions minority class samples into dense, boundary, and noise regions. Moreover, this study integrates this with a progressive sampling scheduler to execute dynamic sampling.
- (3) **A region-guided generation strategy for dynamic sampling.** By originating one end of the synthetic sample in a boundary region and the other in a dense region, the strategy pulls ambiguous samples toward high-confidence dense regions. This effectively mitigates class overlap and reconstructs distinct decision boundaries.

The remainder of this paper is organized as follows. Section 2 reviews the progress and limitations of related work in imbalanced learning. Section 3 introduces the implementation of our proposed model and provides theoretical support for its effectiveness. Section 4 reports the experiments and analyzes the results. Section 5 summarizes the proposed model and discusses future work.

## 2 Related Work

### 2.1 Data-Level Methodologies

Data-level methodologies mitigate class imbalance by either sampling minority class samples or undersampling majority class samples. SMOTE [7], the most foundational approach, generates new samples through stochastic linear interpolation between minority class samples. Augmenting the minority class improves model fitting. Nevertheless, random interpolation often results in low-quality synthetic samples. Several variants have since emerged to improve this process. Han et al. introduced Borderline-SMOTE, which restricts oversampling to minority samples near decision boundaries [19]. He et al. proposed ADASYN, which adaptively allocates the oversampling rate based on the density of surrounding majority class samples [10]. Barua et al. developed MWMOTE, utilizing a two-stage nearest neighbor search to weight informative boundary samples for oversampling [20]. While these methods improve upon basic interpolation, they often rely on K-nearest neighbors. When parent samples reside in regions dominated by the opposing class, these noise points receive excessive attention, leading to the generation of noisy synthetic samples.

To address noise interference and class overlap, recent studies employ clustering and region partitioning strategies. Thakur et al. proposed CBReT, which uses a Gaussian Mixture Model to cluster minority samples and oversamples within each cluster [11]. Furthermore, by calculating the distance between new samples and cluster centroids, this method retains only those samples within a reasonable range. Xie et al. introduced PUMD, which extracts majority class samples by computing density peaks, mitigating the information loss common in traditional cluster-based undersampling

methods [12]. Compared to distance-based strategies, clustering-based more accurately identifies the data distribution; noise samples are typically flagged as outliers or relegated to trivial clusters, preventing them from degrading the oversampling quality.

While effective, CBReT and PUMD primarily target binary classification. Multiclass tasks present more complex decision boundaries that these strategies often struggle to navigate. Consequently, Liu et al. proposed NROMM, which incorporates an adaptive safe embedding mechanism into intra-cluster generation [21]. They further decompose clusters into safe, boundary, and trapped samples based on local density to apply region-specific generation. Shen et al. proposed MCNRO, utilizing a Gaussian Radial Basis Function to calculate class potential energy [22]. By comparing potential energy levels across classes, they partition oversampling regions into high and low potential regions, better accommodating multiclass overlap. Additionally, Xia et al. introduced GBSMOTE, which groups samples using slack variables from the SVM training process [23]. Their study argues that oversampling in a high-dimensional kernel space, rather than in the original geometric space, better alleviates the challenges posed by complex distributions.

Despite these enhancements, data-level methodologies remain limited by their reliance on the dataset's prior distribution. Specifically, these methods configure cluster distributions and partition thresholds based on the original static data. However, the designation of a sample as dense, boundary, or noise should ideally evolve alongside the training process. This lack of dynamic adjustment represents a significant bottleneck for data-level performance.

## 2.2 Algorithm-Level Methodologies

Algorithm-level methodologies encompass cost-sensitive learning and ensemble learning methods. Cost-sensitive methods handle the class imbalance problem by assigning different misclassification costs or sample weights to different classes. Wang et al. proposed AdaBoostNC, which introduces a differentiated cost matrix to penalize minority class misclassifications more heavily [24]. Tang et al. developed TSBQT, a two-stage method that allocates adaptive costs based on classification difficulty to suppress label noise [25]. However, designing reasonable cost matrices or sample weights remains a challenge, especially in multiclass problems [18]. Therefore, compared with cost-sensitive methods, ensemble learning methods have received more favor in algorithm-level research.

Ensemble learning methods construct a strong learner by combining multiple base learners, offering robust generalization and flexibility. Early examples include SMOTEBost [7] and RUSBoost [26], which balance class distributions in each iteration to attenuate the influence of the majority class. In recent years, these methods have been further developed. For example, Rodríguez et al. proposed MultiRandBal. Their study extends the Random Balance strategy to multiclass problems by stochastically assigning class ratios for each base classifier [16]. Zhu et al. proposed OREMBoost. Their study embeds a clean sub-region discovery mechanism into the Boosting process to generate samples exclusively in safe regions [17]. Although these improvement strategies have achieved better performance in multiclass imbalance problems, they do not fully exploit the characteristics of the Boosting process itself. These studies merely incorporate an improved sampling method into the base learners.

In contrast, some other research on ensemble learning have shifted toward adaptively adjusting the model's focus by enhancing the Boosting weight update mechanism. For example, Li et al. proposed AdaBoostAD. Their study integrates the between-class imbalance ratio, the within-class density variable, and the adaptive margin altogether into the AdaBoost framework. By dynamically adjusting sample weights, it augments the model's classification capability on multiclass imbalanced data [18]. Datta et al. proposed LexiBoost, modeling the weight selection problem as a lexicographic linear programming game to balance majority and minority class tradeoffs [19]. Jan et al. proposed JanEnsemble. Their study uses marginal distributions to estimate class preferences and dynamically adjust attention without manual weight configuration [27]. These methods adjust the attention to the majority and minority classes, achieving an adaptive balance mechanism without manually configuring weights. By utilizing statistical information such as density, imbalance ratio, and confidence to furnish real-time feedback to the base learner, these methods are demonstrated substantial adaptability and dynamics.

## 2.3 Limitations of Existing Methodologies

In recent years, data-level methodologies have concentrated on how to enhance sampling quality. Although data-level methodologies have improved sampling quality by transitioning from nearest-neighbor to clustering strategies, these methods remain constrained by the static prior knowledge of the original data. Consequently, they cannot dynamically adjust based on the current state of the training model.

In contrast, algorithm-level methodologies embed imbalanced learning directly into the construction of strong learner. However, many studies merely balance the data before each training epoch. This rudimentary operation fails to synchronize the sampling process with the model's internal optimization. Furthermore, although enhancing weight

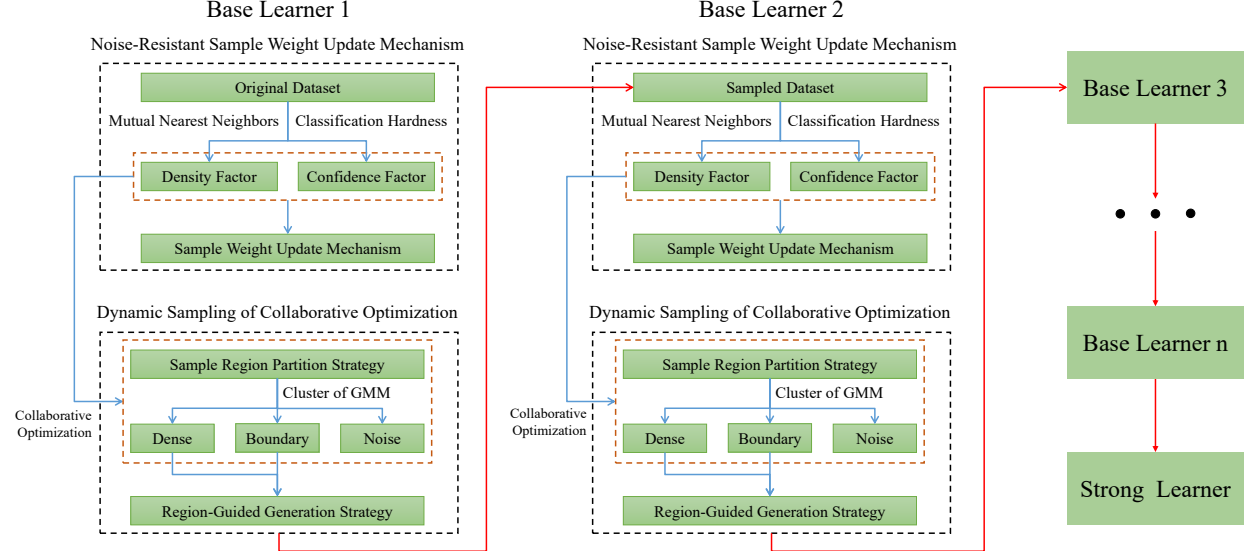


Figure 1: Overall framework of the model proposed in this study. The density factor and confidence factor serve as bridge, they establish a deep coupling between the sample weight update mechanism and the dynamic sampling strategy, enabling the collaborative optimization of imbalanced learning and model training.

update mechanisms is beneficial, simply adjusting weights is often insufficient for complex multiclass datasets that lack distinct decision boundaries. Noise samples and class overlap continue to induce misclassifications that weight adjustment alone cannot surmount.

### 3 Methodology

#### 3.1 Model Overview

To resolve the aforementioned challenges, this study achieves the cooperative optimization of imbalanced learning within the Boosting process. We improve the sample weight update mechanism by introducing a density factor and a confidence factor, overcoming the inherent limitation of traditional AdaBoost, which focuses exclusively on misclassified samples without considering their underlying data distribution or noise characteristics. These factors enable precise sample region partitioning and the design of a progressive sampling scheduler. This scheduler dynamically adjusts sampling quantities in each epoch, synchronizing imbalanced learning with model training. To mitigate noise interference and class overlap, we employ a region-guided generation strategy that pulls ambiguous boundary samples toward high-confidence dense regions, effectively reconstructing distinct decision boundaries. Figure 1 illustrates the overall framework of the model proposed in this study.

#### 3.2 Classic AdaBoost Model

AdaBoost is one of the most prevalent ensemble learning models. It constructs a strong learner by iteratively adjusting sample weights and model weights to integrate multiple base learners. This approach demonstrates superior flexibility and generalization capabilities in both binary and multiclass classification tasks [28]. Given a dataset  $D = \{(x_i, y_i)\}_{i=1}^N$  containing  $N$  samples, where  $x_i \in \mathbb{R}^d$  represents a  $d$ -dimensional feature vector and  $y_i \in \{1, \dots, c\}$  denotes the corresponding class label. AdaBoost trains  $m$  base learners  $\{h_t(\cdot)\}_{t=1}^m$  over  $m$  iterations. Each base learner has a corresponding model weight  $\beta_t$  used to construct the strong learner.

#### 3.3 Noise-Resistant Sample Weight Update Mechanism

Traditional AdaBoost prioritizes hard samples by increasing the weights of misclassified samples. However, because the model evaluates sample importance solely based on the classification error rate, noise samples that are difficult to classify correctly receive progressively larger weights throughout the training process. This limitation is amplified when processing multiclass imbalanced datasets. Traditional AdaBoost forces the model to fit these isolated points, as noise

often mimics hard samples with high errors, leading to overfitting and distorted decision boundaries that encroach on minority class regions.

To mitigate the risk of noise-induced overfitting and ensure the model remains focused on informative data, this study proposes a noise-resistant sample weight update mechanism. By integrating both a density factor and a confidence factor, this mechanism prioritizes samples in dense regions and near decision boundaries while penalizing noise.

### 3.3.1 Density Factor based Mutual Nearest Neighbors

We introduce a density factor based on mutual nearest neighbors to quantify local geometric density. For sample  $x_i$ , if  $x_j$  is in its  $k$ -nearest neighbor set, and  $x_i$  is also in the  $k$ -nearest neighbor set of  $x_j$ , they constitute mutual nearest neighbors. The mutual nearest neighbor set  $\mathcal{N}(x_i)$  of sample  $x_i$  is defined as follows:

$$\mathcal{N}(x_i) = x_j \mid x_j \in \mathcal{N}_k(x_i) \wedge x_i \in \mathcal{N}_k(x_j), \quad (1)$$

where  $\mathcal{N}_k(x_i)$  and  $\mathcal{N}_k(x_j)$  represent the  $k$ -nearest neighbor sets of samples  $x_i$  and  $x_j$ , respectively.

Next, we define the density factor  $\rho_i$  of sample  $x_i$ . The factor  $\rho_i$  quantifies the density of the region where the sample is located through the cardinality of mutual nearest neighbors. It is normalized to the range  $[0, 1]$ :

$$\rho_i = \frac{|\mathcal{N}(x_i)| - \min_j |\mathcal{N}(x_j)|}{\max_j |\mathcal{N}(x_j)| - \min_j |\mathcal{N}(x_j)|}, \quad (2)$$

where  $|\mathcal{N}(x_i)|$  and  $|\mathcal{N}(x_j)|$  represent the cardinalities of the mutual nearest neighbor sets of samples  $x_i$  and  $x_j$ , respectively. When  $\rho_i$  approaches 1, the sample is located in a core high-density region. When  $\rho_i$  approaches 0, the sample is located in a sparse or isolated region.

In this study, the density factor is used for both updating sample weights and partitioning sample regions in the dynamic sampling module. We improve the traditional  $k$ -nearest neighbors by employing mutual nearest neighbors to mitigate density calculation errors triggered by noise. Traditional  $k$ -nearest neighbors establishes a unidirectional relationship based on distance. This leads to erroneous connections with distant samples. Moreover, the asymmetry of traditional  $k$ -nearest neighbors allows noise samples to skew the density evaluation of legitimate samples [29, 30].

Figure 2 visualizes the connection differences between traditional  $k$ -nearest neighbors and mutual nearest neighbors. The significant reduction in the number of edges demonstrates that mutual nearest neighbors effectively filters out noise connections and clarifies the local geometric structure of the data.

### 3.3.2 Confidence Factor based Classification Hardness

The density factor effectively quantifies local sparsity geometrically, it allows the model to distinguish between high-density dense samples and low-density noise. However, density alone cannot distinguish between destructive noise and valuable boundary samples.

To address this, we introduce a confidence factor. This factor measures classification hardness based on the prediction probabilities of the current base learner. We define the classification hardness  $H_i$  of training sample  $x_i$  as:

$$H_i = \frac{1 - p_{y_i}(x_i) + \max_{j \neq y_i} p_j(x_i)}{2}, \quad (3)$$

where  $p_{y_i}(x_i)$  represents the prediction probability of sample  $x_i$  on the true class  $y_i$ , and  $\max_{j \neq y_i} p_j(x_i)$  represents the model's highest prediction probability for its non-true classes.

The classification hardness  $H_i$  ranges from 0 to 1. For samples that are easily classified correctly,  $p_{y_i}(x_i)$  approaches 1, causing  $H_i$  to approach 0. For difficult ones,  $H_i$  approaches 1. A value of  $H_i$  near 0.5 indicates ambiguity, where the samples typically lie near the decision boundaries.

To utilize hardness for weight adjustment, we map  $H_i$  to a confidence factor  $\delta_i$  using a Gaussian function:

$$\delta_i = 1 - \exp\left(-\frac{(H_i - \mu_H)^2}{2\sigma_H^2}\right), \quad (4)$$

where  $\mu_H$  and  $\sigma_H$  represent the mean and standard deviation of classification hardness across all training samples.

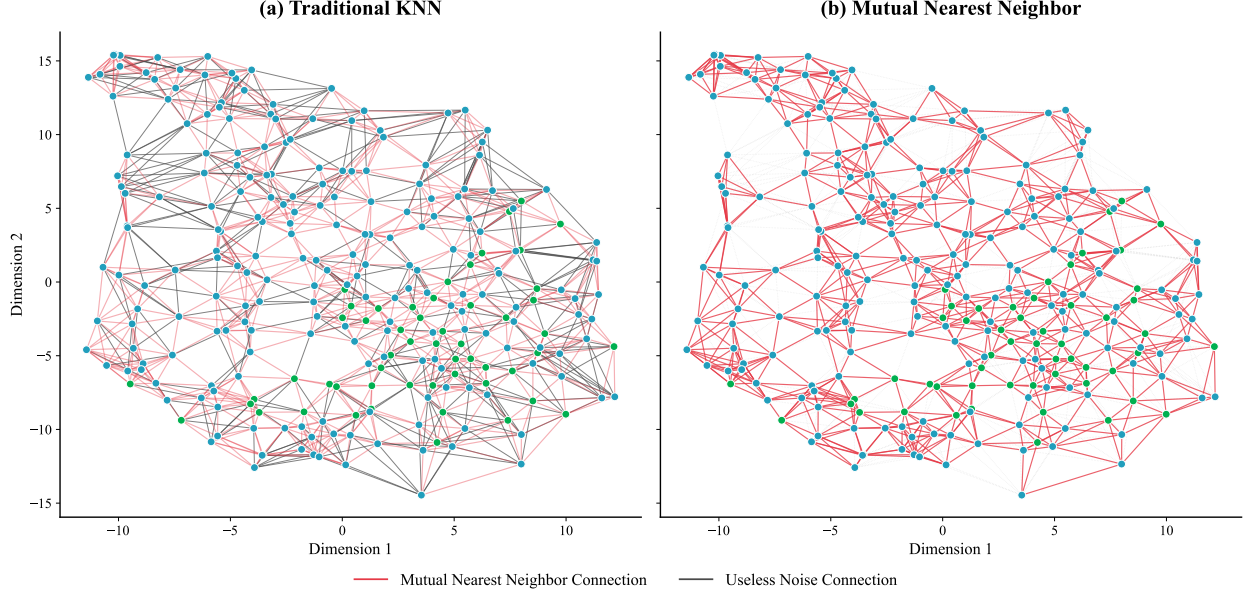


Figure 2: Comparison of connectivity between  $k$ -nearest neighbors and mutual nearest neighbors with  $k=10$ . The  $k$ -nearest neighbors establishes 2,670 edges, the mutual nearest neighbors establishes only 1,141 edges.

When a sample’s hardness approaches the mean,  $\delta_i$  approaches 0, indicating minimum model confidence. This characterizes ambiguous boundary samples. Conversely, when  $\delta_i$  approaches 1, the sample is either extremely easy or extremely hard to classify. These extremes generally correspond to simple samples or noise, respectively.

### 3.3.3 Sample Weight Update Formula

The density factor and confidence factor characterize samples from two complementary perspectives: geometric structure and classification hardness. Relying on a single factor is insufficient. Specifically, the density factor identifies sparse samples but cannot determine whether the sparsity stems from meaningless noise or valuable boundary samples, because they are all difficult to classify correctly. Conversely, relying solely on the confidence factor mirrors traditional AdaBoost, emphasizing hard samples excessively and often leading to overfitting on noise.

The cooperative action of these two factors is key to achieving noise resistance and imbalanced learning. The density factor partitions samples into dense and non-dense regions. To distinguish between isolated noise samples and ambiguous boundary samples, the non-dense regions are further divided into boundary and noise regions using the confidence factor.

We fuse the density factor and confidence factor to construct a novel sample weight update mechanism. Given the sample weight  $w^{(t)}$  in the  $t$ -th epoch, the updated weight  $w^{(t+1)}$  is defined as:

$$\omega^{(t+1)} = \exp\left(-\delta^{(t)} \cdot (1 - \rho^{(t)})\right) \cdot \omega^{(t)} \cdot \exp\left(-\beta^{(t)} \cdot \mathbb{I}[h_t(x_i) = y_i]\right), \quad (5)$$

where  $\rho^{(t)}$  and  $\delta^{(t)}$  represent the density factor and confidence factor of the  $t$ -th epoch, respectively.  $\mathbb{I}[h_t(x_i) = y_i]$  represents the indicator function, which is 1 when the prediction of the base learner  $h_t$  for sample  $x_i$  is correct, and 0 otherwise.  $\beta^{(t)}$  is the voting weight of AdaBoost. Its calculation follows the concept of traditional AdaBoost, the lower the classification error rate of the base learner, the larger its weight:

$$\beta^{(t)} = \frac{1}{2} \ln\left(\frac{1 - \epsilon_t}{\epsilon_t}\right) = \frac{1}{2} \ln\left(\frac{\sum_{h_t(x_i) = y_i} \omega^{(t)}(x_i, y_i)}{\sum_{h_t(x_i) \neq y_i} \omega^{(t)}(x_i, y_i)}\right), \quad (6)$$

where  $\epsilon_t$  represents the classification error rate of the  $t$ -th epoch base learner.

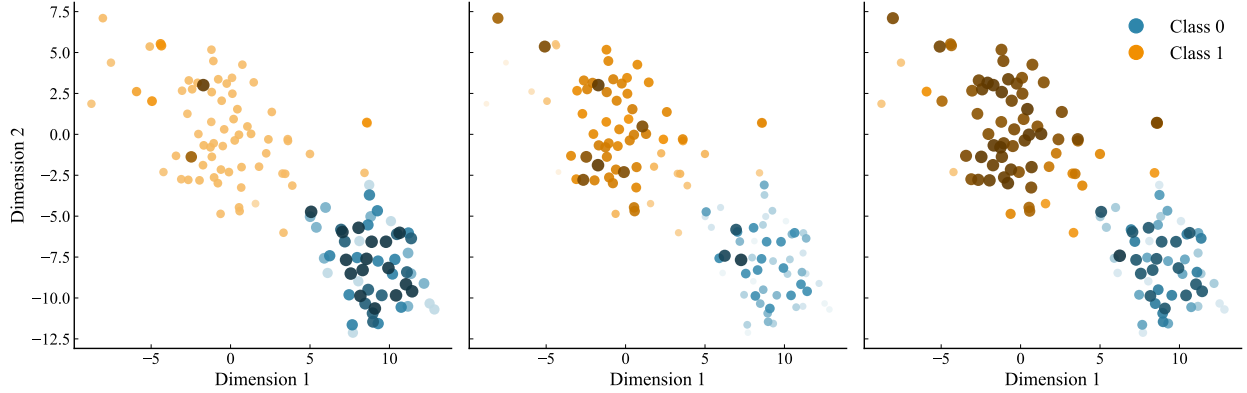


Figure 3: Evolution of sample weights during training process, darker shades indicate higher weights.

Figure 3 visualizes the changes in sample weights as the number of iterations increases. Samples located in dense regions receive increased weights because they provide valuable structural information for model fitting. Conversely, the mechanism reduces the weights of noisy samples situated far from the cluster centers. Meanwhile, boundary samples receive progressively greater attention across iterations to reconstruct clear decision boundaries. This targeted weighting strategy ensures that the model focuses on high-value samples while remaining robust to noise.

The pseudocode for the improved sample weight update mechanism is shown in Algorithm 1.

---

**Algorithm 1:** Noise-Resistant Sample Weight Update Mechanism

---

**Input:** Dataset  $D = \{(x_i, y_i)\}_{i=1}^N$ , Base learner  $h_t$ , Sample weights  $\omega^{(t)}$ , Neighbor count  $k$

**Output:** Updated sample weights  $\omega^{(t+1)}$

```

1 Stage 1: Compute Density Factor;
2 for  $i = 1$  to  $N$  do
3   | Identify mutual nearest neighbor set  $\mathcal{N}(x_i)$   $\triangleright$  Eq.(1);
4   | Compute density factor  $\rho_i^{(t)}$  based on mutual nearest neighbor  $\triangleright$  Eq.(2);
5 end
6 Stage 2: Compute Confidence Factor;
7 Initialize hardness vector  $\mathbf{H} = [H_1, \dots, H_N]$ ;
8 for  $i = 1$  to  $N$  do
9   | Obtain prediction probabilities  $p(x_i)$  from  $h_t$ ;
10  | Compute classification hardness  $H_i$  based on prediction probabilities  $\triangleright$  Eq.(3);
11 end
12 Compute mean  $\mu_H$  and standard deviation  $\sigma_H$  of vector  $\mathbf{H}$ ;
13 for  $i = 1$  to  $N$  do
14   | Compute confidence factor  $\delta_i^{(t)}$  using Gaussian mapping  $\triangleright$  Eq.(4);
15 end
16 Stage 3: Update Sample Weights;
17 Compute base learner error rate  $\epsilon_t$ ;
18 Compute voting weight  $\beta^{(t)}$   $\triangleright$  Eq.(6);
19 for  $i = 1$  to  $N$  do
20   | Update weight  $\omega_i^{(t+1)}$  by fusing  $\rho_i^{(t)}$ ,  $\delta_i^{(t)}$ , and  $\beta^{(t)}$   $\triangleright$  Eq.(5);
21 end
22 Normalize weights  $\omega^{(t+1)}$  such that  $\sum_{i=1}^N \omega_i^{(t+1)} = 1$ ;
23 return  $\omega^{(t+1)}$ 

```

---

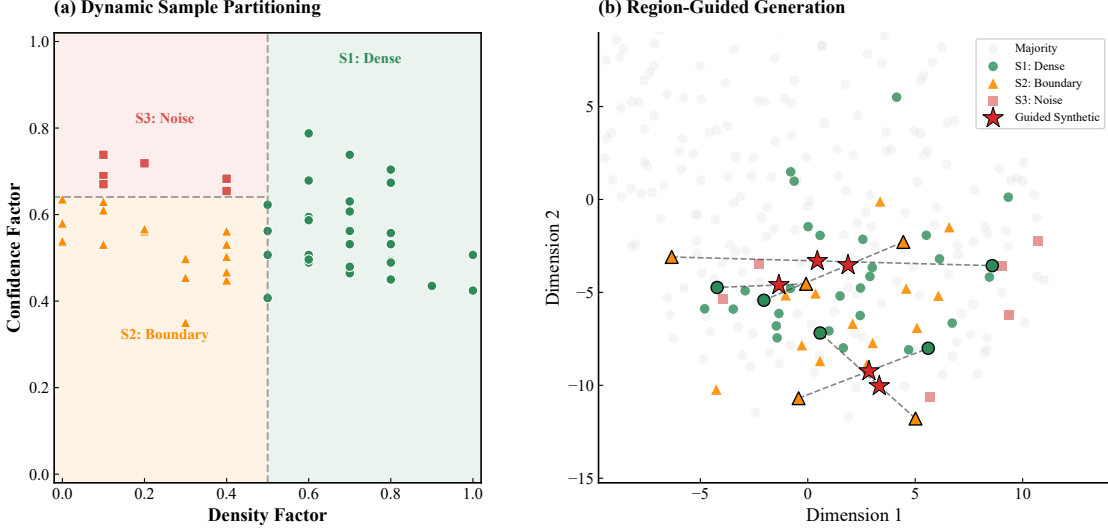


Figure 4: Schematic diagram of dynamic sampling under collaborative optimization.

### 3.4 Dynamic Sampling through Collaborative Optimization

Traditional algorithm-level methodologies typically combine data sampling and model training in a simple manner, isolating the sampling process from the ensemble learning model and limiting the imbalanced learning performance. To address this issue, this study designs a dynamic sampling strategy based on the density factor and confidence factor.

Furthermore, to overcome the drawbacks of blind interpolation in traditional oversampling methods, we design a region-guided generation strategy. This strategy requires that one parent sample originates from the boundary region and the other from the dense region, drawing ambiguous boundary samples toward the dense region. In addition, we propose a progressive sampling scheduler to manage the synthesis process. This scheduler adaptively controls the number of synthetic samples generated for each base learner and each cluster by incorporating both the density factor and the confidence factor.

#### 3.4.1 Sample Region Partitioning Strategy

Traditional sampling methods typically perform random sampling or undersampling across the entire sample space. These methods often ignore local distribution heterogeneity, which can degrade the quality of generated samples or reduce the effectiveness of sample elimination. To address this, we first partition the minority class into multiple clusters. Sample region partitioning and synthesis are then performed independently within each cluster.

When oversampling class  $c$ , it is treated as the minority class. All other classes with larger sample sizes than class  $c$  are categorized as the majority class. Within each cluster  $s$ , the rules for sample region partitioning are defined as follows:

$$\{(x_i, y_i)\}_s \in \begin{cases} \mathcal{S}_1, & \rho_i \geq \rho_0, \\ \mathcal{S}_2, & \rho_i < \rho_0 \text{ and } H_i > \mu_H - \sigma_H, \\ \mathcal{S}_3, & \rho_i < \rho_0 \text{ and } H_i \leq \mu_H - \sigma_H, \end{cases} \quad s = 1, \dots, g, \quad (7)$$

where  $\rho_i$  denotes the density factor of the  $i$ -th sample within cluster  $s$ ,  $g$  represents the total number of clusters, which is determined using the Bayesian Information Criterion [31]. Additionally,  $\rho_0$  serves as a predefined density threshold, and  $\mu_H$  and  $\sigma_H$  represent the mean and standard deviation of sample confidence, respectively. Based on these parameters, the equation partitions the samples within each cluster into the following three regions:

- (1) **Dense Region  $\mathcal{S}_1$** : High density and far from the cluster boundaries. These samples are typically easy to classify.
- (2) **Boundary Region  $\mathcal{S}_2$** : Lower density but higher confidence. These samples are typically located near the cluster boundaries and easily confused with other classes.
- (3) **Noise Region  $\mathcal{S}_3$** : Both density and confidence are lower. These samples are typically far from the cluster center and may represent noise far from the decision boundaries.

This clustering-based partitioning strategy ensures targeted sampling operations. It provides a reliable guarantee for generating high-quality samples that maintain similar distributions, thereby clarifying decision boundaries. Furthermore, using the mean and standard deviation of the confidence factor as criteria in Eq.(7) reduces the need for manual threshold tuning. This setting also enables the adaptive determination of parameters based on the specific distribution of the dataset.

---

**Algorithm 2:** Dynamic Sampling through Collaborative Optimization

---

**Input:** Minority class dataset  $D_c = \{(x_i, y_i)\}$ , Current epoch  $t$ , Total epochs  $m$ , Density threshold  $\rho_0$   
**Output:** Sampled dataset  $D'_c$

```

1 Stage 1: Adaptive Clustering
2 Determine optimal cluster count  $g$  via Bayesian Information Criterion
3 Decompose  $D_c$  into  $g$  clusters  $\{C_1, \dots, C_g\}$  using Gaussian Mixture Model
4 Stage 2: Sample Region Partitioning
5 for each cluster  $s \in \{1, \dots, g\}$  do
6   for each sample  $x_i \in C_s$  do
7     if  $\rho_i \geq \rho_0$  then
8       | Assign  $x_i \rightarrow$  Dense Region
9     else if  $\rho_i < \rho_0$  and  $H_i > \mu_H - \sigma_H$  then
10      | Assign  $x_i \rightarrow$  Boundary Region
11    else
12      | Assign  $x_i \rightarrow$  Noise Region
13  end
14 end
15 Stage 3: Dynamic Sampling Allocation
16 Compute the base learner target sampling weight  $O_t \triangleright$  Eq.(10)
17 for each cluster  $s \in \{1, \dots, g\}$  do
18   | Compute the target sampling weight  $P_s \triangleright$  Eq.(9)
19   | Calculate the total target sample quantity  $T_{st} \triangleright$  Eq.(8)
20 end
21 Stage 4: Region-Guided Generation
22 Initialize synthetic set  $x_{syn} = \emptyset$ 
23 for each cluster  $s \in \{1, \dots, g\}$  do
24   while  $|x_{syn}| < \text{allocated count for } s$  do
25     | Select parent  $x_a$  from Boundary Region and  $x_b$  from Dense Region
26     | Generate  $x_{new} \triangleright$  Eq.(11)
27     | Add  $x_{new}$  to  $x_{syn}$ 
28   end
29 end
30  $D'_c \leftarrow D_c \cup x_{syn}$ 
31 return  $D'_c$ 

```

---

### 3.4.2 Region-Guided Synthetic Sample Generation

Traditional sampling methods typically balance datasets by increasing the minority class count to match the majority class in a single step. In contrast, we propose a progressive sampling scheduler that allocates a specific sampling quantity to each training epoch.

The progressive sampling scheduler integrates dynamic sampling directly into the iterative training process. Specifically, it first determines the total target sampling quantity for each class, and then dynamically assigns sampling weights to

different clusters across epochs. These weights are adaptively determined based on both cluster-level and base-learner target sampling requirements.

For the currently processed class  $c$  in the  $t$ -th epoch, the target sampling quantity  $T_{st}$  of cluster  $s$  is calculated as:

$$T_{st} = \lfloor P_s \cdot O_t \cdot (\max_{c'} N(c') - N(c)) \rfloor, \quad s = 1, \dots, g, \quad t = 1, \dots, m, \quad (8)$$

where  $\max_{c'} N(c')$  represents the total target sample quantity required for the class  $c$ ,  $\lfloor \cdot \rfloor$  represents the floor function,  $c'$  represents the majority class,  $O_t$  represents the target sampling weight of the  $t$ -th base learner. In addition,  $P_s$  represents the target sampling weight of cluster  $s$ , it is calculated as follows:

$$P_s = \frac{\rho_s^{avg} \cdot |N_s|}{\sum_{s=1}^g \rho_s^{avg} \cdot |N_s|}, \quad (9)$$

where  $\rho_s^{avg}$  represents the average density factor of the  $s$ -th cluster, and  $|N_s|$  represents the sample quantity of the  $s$ -th cluster.

The base learner target sampling weight  $O_t$  is calculated as:

$$O_t = \frac{\tan\left(\frac{m-t}{m-1} \cdot \frac{\pi}{4}\right)}{\sum_{t=1}^m \tan\left(\frac{m-t}{m-1} \cdot \frac{\pi}{4}\right)}, \quad (10)$$

where  $m$  is the total number of AdaBoost iterations.

The cluster target sampling weight  $P_s$  accounts for both sample density and cluster size, it assigns higher weights to clusters with high density and large sample counts, as these clusters typically contain high-quality samples and provide higher fitting value.

Meanwhile, the base learner target sampling weight  $O_t$  is determined by a tangent function. This function allocates larger sampling weights during the early stages of training. As training progresses, the weight gradually decreases. This strategy allows the model to quickly compensate for the minority class deficit initially. As the decision boundaries stabilize, the sampling intensity decreases, ensuring a smoother and more effective learning process.

Finally, after determining the target sampling quantity  $T_{st}$  for cluster  $s$  in the  $t$ -th epoch, we perform region-guided sample synthesis as follows:

$$x_{new} = x_a + \lambda(x_b - x_a), \quad x_a \in \mathcal{S}_2, \quad x_b \in \mathcal{S}_1, \quad \lambda \in \mathcal{U}(0, 1) \quad (11)$$

where  $x_a$  and  $x_b$  represent parent samples from the boundary region and dense region, respectively.

Figure 4 illustrates the dynamic sampling strategy under cooperative optimization. Specifically, Figure 4(a) details the sample region partitioning strategy, which categorizes samples into three distinct regions based on their density factor and confidence factor. Figure 4(b) depicts the region-guided sample synthesis strategy. This strategy locks the boundary samples and performs guided interpolation toward dense samples, thereby generating synthetic samples with high confidence. The pseudocode for the dynamic sampling through collaborative optimization is shown in Algorithm 2.

### 3.5 Theoretical Derivation of Model Effectiveness

Traditional oversampling methods often introduce noise, which hinders the stability of the model during training. These methods typically treat all synthetic samples as equally beneficial, often leading to ambiguous decision boundaries easily. To address this limitation, we propose a region-guided strategy, the synthetic samples should be generated in high-quality regions to maximize their benefit. Specifically, the proposed strategy minimizes the expected loss and effectively reconstructs distinct decision boundaries by guiding the synthesis process toward the density region.

To justify this mechanism, we demonstrate how integrating the density factor and confidence factor into the sample weight update is equivalent to minimizing a regularized exponential loss.

We define a strong learner at epoch  $t$  as  $F_t(x) = \sum_{\tau=1}^t \beta_\tau h_\tau(x)$ . To account for local distribution heterogeneity and sample quality, we propose a global objective function  $\mathcal{L}_t$ :

$$\mathcal{L}_t = \sum_{i=1}^N \left[ \prod_{\tau=1}^t e^{-\delta_i^{(\tau)}(1-\rho_i^{(\tau)})} \right] e^{-y_i F_t(x_i)}. \quad (12)$$

Here,  $\delta_i$  and  $\rho_i$  weight the importance of each sample's contribution to the total loss. Following the forward stagewise additive modeling approach, the learner at epoch  $t$  is  $F_t(x_i) = F_{t-1}(x_i) + \beta_t h_t(x_i)$ . Substituting this into Eq.(12) yields:

$$\mathcal{L}_t = \sum_{i=1}^N \left[ \prod_{\tau=1}^{t-1} e^{-\delta_i^{(\tau)}(1-\rho_i^{(\tau)})} \cdot e^{-y_i F_{t-1}(x_i)} \right] \cdot e^{-\delta_i^{(t)}(1-\rho_i^{(t)})} \cdot e^{-y_i \beta_t h_t(x_i)}. \quad (13)$$

The term within the square brackets represents the unnormalized weight  $w_{t,i}$  assigned to the  $i$ -th sample at the beginning of epoch  $t$ . Thus, the objective can be rewritten as:

$$\mathcal{L}_t = \sum_{i=1}^N w_{t,i} \cdot e^{-\delta_i^{(t)}(1-\rho_i^{(t)})} \cdot e^{-y_i \beta_t h_t(x_i)}. \quad (14)$$

To find the optimal model weight  $\beta_t$  that minimizes  $\mathcal{L}_t$ , we take the partial derivative with respect to  $\beta_t$ :

$$\frac{\partial \mathcal{L}_t}{\partial \beta_t} = \sum_{i=1}^N w_{t,i} \cdot e^{-\delta_i^{(t)}(1-\rho_i^{(t)})} \cdot (-y_i h_t(x_i)) \cdot e^{-y_i \beta_t h_t(x_i)} = 0. \quad (15)$$

Next, we split the summation based on whether the base learner  $h_t$  classifies the sample correctly. Let  $\alpha_{i,t} = w_{t,i} \cdot e^{-\delta_i^{(t)}(1-\rho_i^{(t)})}$ , since  $y_i, h_t(x_i) \in \{-1, 1\}$ , the product  $y_i h_t(x_i)$  yields the following properties:

- (1) Correct classification ( $y_i = h_t(x_i)$ ):  $y_i h_t(x_i) = 1$ , thus the term becomes  $-\alpha_{i,t} e^{-\beta_t}$ .
- (2) Incorrect classification ( $y_i \neq h_t(x_i)$ ):  $y_i h_t(x_i) = -1$ , thus the term becomes  $\alpha_{i,t} e^{\beta_t}$ .

Substituting these into the derivative equation:

$$-\sum_{i:y_i=h_t(x_i)} \alpha_{i,t} e^{-\beta_t} + \sum_{i:y_i \neq h_t(x_i)} \alpha_{i,t} e^{\beta_t} = 0. \quad (16)$$

Rearranging the terms gives:

$$e^{\beta_t} \sum_{i:y_i \neq h_t(x_i)} \alpha_{i,t} = e^{-\beta_t} \sum_{i:y_i=h_t(x_i)} \alpha_{i,t}. \quad (17)$$

Multiplying both sides by  $e^{\beta_t}$  and then taking the natural logarithm:

$$e^{2\beta_t} = \frac{\sum_{i:y_i=h_t(x_i)} \alpha_{i,t}}{\sum_{i:y_i \neq h_t(x_i)} \alpha_{i,t}} \implies 2\beta_t = \ln \left( \frac{\sum_{i:y_i=h_t(x_i)} \alpha_{i,t}}{\sum_{i:y_i \neq h_t(x_i)} \alpha_{i,t}} \right). \quad (18)$$

Substituting  $\alpha_{i,t}$  back, we obtain the final analytical expression for  $\beta_t$ :

$$\beta_t = \frac{1}{2} \ln \left( \frac{\sum_{i:y_i=h_t(x_i)} w_{t,i} \cdot e^{-\delta_i^{(t)}(1-\rho_i^{(t)})}}{\sum_{i:y_i \neq h_t(x_i)} w_{t,i} \cdot e^{-\delta_i^{(t)}(1-\rho_i^{(t)})}} \right). \quad (19)$$

To summarize, this derivation confirms that our model achieves a deep coupling between sample quality and ensemble optimization. The analytic solution for  $\beta_t$  proves that the noise-resistant update is equivalent to minimizing a regularized exponential loss. Within this process,  $\delta_i$  and  $\rho_i$  act as adaptive regularization terms that penalize outliers, thereby maintaining the mathematical rigor of Boosting while enhancing robustness against noise.

## 4 Experiments and Discussion

### 4.1 Experimental Setting

In this study, Python 3.12 was used as the programming language for the implementation of the code, with all necessary dependencies installed through the Anaconda distribution, including scikit-learn (version 1.5.1) for the implementation of the machine learning algorithms, Pandas (version 2.2.2) for the data processing, and numerical operations with NumPy (version 1.26.4). All experimental evaluations were conducted on a Windows 11 (64-bit) platform equipped with an AMD Ryzen 5 6600H processor and 16GB RAM.

### 4.2 Datasets

To ensure statistical significance and generalization, we selected 20 classification datasets from the KEEL repository [32]. These datasets vary widely in their imbalance ratios, feature dimensions, and class counts, covering diverse scenarios, ranging from low to high dimensionality and from mild to extreme imbalance. Table 1 summarizes the characteristics of these datasets. We split each dataset into training and testing sets using an 80:20 ratio. In our analysis, `n_Samples`, `n_Features`, and `n_Classes` denote the total number of samples, features, and classes, respectively. The `Imbalance_Ratio` is defined as the ratio of the majority class size to the minority class size.

Table 1: Statistical information of the investigated datasets.

Dataset	n_Samples	n_Features	n_Classes	Imbalance_Ratio
automobile	156	25	5	3.69
car	1728	6	4	18.62
contraceptive	1473	9	3	1.89
dermatology	358	34	6	5.60
ecoli2	336	7	2	5.46
glass	214	9	6	8.44
haberman	306	3	2	2.78
hayesroth	132	4	3	1.70
heart	267	44	2	3.86
led7digit	500	7	10	1.54
newthyroid	215	5	3	5.00
newthyroid1	215	5	2	5.14
newthyroid2	215	5	2	5.14
pageblocks	545	10	4	61.50
shuttle	2173	9	4	284.33
tae	151	5	3	1.06
thyroid	720	21	3	39.18
vehicle	846	18	4	1.10
wine	178	13	3	1.48
zoo	101	16	7	10.25

### 4.3 Baselines

We evaluated the proposed model against eight state-of-the-art imbalanced learning methods. These baselines include five algorithm-level models and three data-level models. To ensure a fair comparison, all data-level models utilized AdaBoost as the base classifier, and the number of base learners was fixed at 50 for all models. We performed hyperparameter tuning via 5-fold cross-validation on the training set, Bayesian optimization was employed with 50 iterations [33–35].

Table 2 provides a detailed summary of these baseline models. Table 3 lists the hyperparameter search ranges, and Table 4 presents the final settings. We employed Accuracy, Weighted F1-score, G-Mean, and AUC as evaluation metrics. These metrics provide a comprehensive assessment of model performance on multiclass imbalanced datasets.

### 4.4 Performance Comparison

This section evaluates the comprehensive performance of the proposed model on multiclass imbalanced tasks. Tables 5 through 8 report the Accuracy, Weighted F1-score, G-Mean, and AUC for all models, respectively. Table 9 summarizes the average rankings. The bolded values represent the best performance.

Table 2: Comparison of baselines for imbalanced learning.

Method	Category	Year	Brief Description
AdaBoostAD[18]	Algorithm-level	2024	Adaptive weighting mechanism based on class imbalance ratios and local density
AdaBoostNC[24]	Algorithm-level	2012	Negative correlation penalty to enhance base classifier diversity
LexiBoost[19]	Algorithm-level	2020	Lexicographic optimization for automatic inter-class trade-off balancing
MultiRandBal[16]	Algorithm-level	2020	Random undersampling and oversampling with diverse prior distributions
OREMBoost[17]	Algorithm-level	2023	Safe sub-region expansion for online sample generation
GBSMOTE[23]	Data-level	2023	Granular ball-based oversampling in hypersphere space
MCNRO[21]	Data-level	2024	Neighborhood re-partitioning for multiclass scenarios
NROMM[22]	Data-level	2023	One-sided minimum margin with clustering-based denoising

Table 3: Hyperparameter search space and descriptions.

Model	Hyperparameter	Search Space	Type	Description
AdaBoostAD	max_depth	[1, 50]	Integer	Max depth of base learner
AdaBoostNC	lambda_param	[1, 10]	Integer	Diversity penalty weight
	max_depth	[1, 50]	Integer	Max depth of base learner
GBSMOTE	C	[0.1, 5.0]	Float (Log-uniform)	Regularization coefficient
	gamma	['scale', 'auto']	Categorical	RBF kernel coefficient
	max_depth	[1, 50]	Integer	Max depth of base learner
LexiBoost	max_depth	[1, 50]	Integer	Max depth of base learner
MCNRO	k	[3, 9]	Integer	Number of nearest neighbors
	epsilon	[0.1, 0.9]	Float (Step 0.05)	Overlap threshold
	max_depth	[1, 50]	Integer	Max depth of base learner
MultiRandBal	max_depth	[1, 50]	Integer	Max depth of base learner
NROMM	max_depth	[1, 50]	Integer	Max depth of base learner
OREMBoost	q	[3, 10]	Integer	Queue parameter
Ours	k	[2, 20]	Integer	Number of mutual nearest neighbors
	max_depth	[1, 50]	Integer	Max depth of base learner
	density_threshold	[0.1, 0.9]	Float (Step 0.05)	Density partitioning threshold

As shown in Table 5, the proposed model achieves the highest classification accuracy on most datasets. Even on datasets where it does not rank first, such as dermatology and ecoli2, the model consistently ranks within the top three. Table 6 presents the Weighted F1-score results, which follow the same trends as classification accuracy. Notably, on the vehicle dataset, our model achieves an F1-score of 0.810. This is significantly higher than the second-best method, OREMBoost, which reaches 0.742. Table 7 reports the G-Mean performance, which reflects the model's ability to balance the classification of minority and majority classes. The results show that the proposed model maintains high G-Mean values across various multiclass tasks. Table 8 provides the AUC score comparison. Although the model achieves the best AUC performance on fewer datasets compared to other metrics, it still ranks first on 11 datasets.

As summarized in Table 9, the proposed model achieves average rankings of 1.62, 1.69, 1.81, and 2.69 across the four metrics. In contrast, the best baseline, OREMBoost, achieves average rankings of 3.81, 3.81, 4.12, and 5.00. This consistent performance demonstrates the robustness of our model across different imbalance ratios and feature dimensions.

This superior performance stems from the proposed cooperative optimization mechanism, which addresses the limitations of existing methods. Traditional data-level methods rely on static priors, which makes them susceptible to isolated noise and distribution deviations. In contrast, our dynamic sampling strategy utilizes mutual nearest neighbor information to suppress noise weights. This approach ensures that generated samples are high-quality and discriminative.

Furthermore, existing algorithm-level methods often focus on numerical weight adjustments without explicitly utilizing geometric distributions. Our model uses a region-guided strategy to reconstruct clear decision boundaries, effectively

Table 4: Hyperparameter settings for each model.

Dataset	AdaBoostAD	AdaBoostNC	GBSMOTE	LightGBM	MCNRO	MultiRandBal	NROMM	OREMBost	Ours
automobile	max_depth=33	max_depth=7 lambda_param=1	max_depth=30 C=1.9 gamma=scale	max_depth=8	max_depth=33 k=9 epsilon=0.5	max_depth=33 k=4 rho_threshold=50	max_depth=8 q=8	max_depth=8 k=16 max_depth=4 density_threshold=0.65	max_depth=8 k=5 max_depth=10
car	max_depth=8	max_depth=7 lambda_param=1	max_depth=40 C=0.22 gamma=scale	max_depth=33	max_depth=33 k=9 epsilon=0.5	max_depth=7 k=3 rho_threshold=15	max_depth=23 q=5	max_depth=8 k=14 max_depth=4 density_threshold=0.1	max_depth=3 k=5 density_threshold=0.3
contraceptive	max_depth=33	max_depth=8 lambda_param=7	max_depth=23 C=0.35 gamma=scale	max_depth=7	max_depth=8	max_depth=35 k=7 rho_threshold=55	max_depth=7 q=3	max_depth=8 k=14 max_depth=3 density_threshold=0.9	max_depth=3 k=5 density_threshold=0.3
dermatology	max_depth=33	max_depth=8 lambda_param=7	max_depth=33 C=4.94 gamma=auto	max_depth=7	max_depth=8	max_depth=35 k=4 rho_threshold=10	max_depth=33 q=10	max_depth=7 k=6 max_depth=5 density_threshold=0.9	max_depth=5 k=6 density_threshold=0.9
ecoli2	max_depth=33	max_depth=33 lambda_param=10	max_depth=39 C=0.21 gamma=auto	max_depth=1	max_depth=23 k=5 epsilon=0.85	max_depth=1 k=7 rho_threshold=50	max_depth=33 q=3	max_depth=8 k=9 max_depth=21	max_depth=3 k=9 density_threshold=0.3
glass	max_depth=8	max_depth=33 lambda_param=10	max_depth=33 C=4.94 gamma=auto	max_depth=33	max_depth=33 k=9 epsilon=0.5	max_depth=33 k=4 rho_threshold=50	max_depth=33 q=8	max_depth=7 k=8 max_depth=5 density_threshold=0.15	max_depth=5 k=8 density_threshold=0.3
haberman	max_depth=8	max_depth=30 lambda_param=8	max_depth=8 C=1.54 gamma=auto	max_depth=1	max_depth=35 k=7 epsilon=0.85	max_depth=39 k=4 rho_threshold=10	max_depth=40 q=4	max_depth=25 k=9 max_depth=30	max_depth=25 k=15 density_threshold=0.8
hayesroth	max_depth=33	max_depth=33 lambda_param=10	max_depth=33 C=4.94 gamma=auto	max_depth=1	max_depth=33 k=9 epsilon=0.5	max_depth=33 k=3 rho_threshold=50	max_depth=26 q=8	max_depth=8 k=8 max_depth=5 density_threshold=0.15	max_depth=5 k=8 density_threshold=0.3
heart	max_depth=33	max_depth=7 lambda_param=1	max_depth=8 C=1.54 gamma=auto	max_depth=33	max_depth=33 k=9 epsilon=0.5	max_depth=33 k=3 rho_threshold=15	max_depth=33 q=10	max_depth=8 k=9 max_depth=20	max_depth=8 k=15 max_depth=30
led7digit	max_depth=33	max_depth=33 lambda_param=10	max_depth=50 C=0.29 gamma=auto	max_depth=50	max_depth=33 k=3 epsilon=0.2	max_depth=39 k=4 rho_threshold=60	max_depth=26 q=8	max_depth=3 k=4 max_depth=3	max_depth=25 k=16 max_depth=3
newthyroid1	max_depth=33	max_depth=33 lambda_param=10	max_depth=39 C=0.21 gamma=auto	max_depth=1	max_depth=7 k=3 epsilon=0.2	max_depth=33 k=7 rho_threshold=50	max_depth=33 q=10	max_depth=6 k=8 max_depth=17	max_depth=6 k=8 density_threshold=0.9
newthyroid2	max_depth=33	max_depth=33 lambda_param=10	max_depth=33 C=4.94 gamma=auto	max_depth=33	max_depth=33 k=9 epsilon=0.5	max_depth=33 k=7 rho_threshold=60	max_depth=33 q=8	max_depth=8 k=4 max_depth=1	max_depth=8 k=4 density_threshold=0.65
newthyroid3	max_depth=33	max_depth=33 lambda_param=10	max_depth=33 C=4.94 gamma=auto	max_depth=33	max_depth=33 k=9 epsilon=0.5	max_depth=33 k=7 rho_threshold=55	max_depth=33 q=10	max_depth=8 k=8 max_depth=17	max_depth=8 k=8 density_threshold=0.2
pageblocks	max_depth=33	max_depth=33 lambda_param=10	max_depth=33 C=1.9 gamma=scale	max_depth=33	max_depth=33 k=9 epsilon=0.5	max_depth=33 k=3 rho_threshold=15	max_depth=26 q=3	max_depth=7 k=14 max_depth=50	max_depth=7 k=14 max_depth=50
shuttle	max_depth=33	max_depth=33 lambda_param=10	max_depth=33 C=4.94 gamma=auto	max_depth=33	max_depth=33 k=9 epsilon=0.5	max_depth=33 k=7 rho_threshold=50	max_depth=33 q=10	max_depth=5 k=14 max_depth=50	max_depth=5 k=14 max_depth=50
tae	max_depth=8	max_depth=8 lambda_param=7	max_depth=33 C=4.94 gamma=auto	max_depth=8	max_depth=33 k=7 epsilon=0.7	max_depth=8 k=4 rho_threshold=45	max_depth=33 q=8	max_depth=16 k=10 max_depth=85	max_depth=8 k=5 max_depth=13
thyroid	max_depth=7	max_depth=33 lambda_param=10	max_depth=33 C=4.94 gamma=auto	max_depth=33	max_depth=7 k=3 epsilon=0.2	max_depth=33 k=3 rho_threshold=45	max_depth=33 q=10	max_depth=13 k=5 max_depth=65	max_depth=13 k=6 max_depth=65
vehicle	max_depth=8	max_depth=33 lambda_param=10	max_depth=8 C=1.54 gamma=auto	max_depth=8	max_depth=33 k=7 epsilon=0.7	max_depth=33 k=4 rho_threshold=10	max_depth=26 q=8	max_depth=9 k=5 max_depth=8	max_depth=9 k=5 max_depth=8
wine	max_depth=33	max_depth=33 lambda_param=10	max_depth=33 C=4.94 gamma=auto	max_depth=33	max_depth=7 k=3 epsilon=0.2	max_depth=33 k=3 rho_threshold=15	max_depth=26 q=8	max_depth=2 k=12 max_depth=45	max_depth=2 k=12 max_depth=45
zoo	max_depth=33	max_depth=33 lambda_param=10	max_depth=33 C=4.94 gamma=auto	max_depth=33 k=9 epsilon=0.5	max_depth=33 k=9 rho_threshold=35	max_depth=33 k=10 rho_threshold=35	max_depth=33 q=10	max_depth=3 k=14 max_depth=30	max_depth=3 k=14 max_depth=30

mitigating class overlap. Overall, these quantitative results validate the effectiveness of the model in handling complex data distributions.

Table 5: Comparison of Accuracy and Rank.

Dataset	AdaBoostAD	AdaBoostNC	GBSMOTE	LexiBoost	MCNRO	MultiRandBal	NROMM	OREMBoost	Ours
automobile	0.875 <sub>4</sub>	0.906 <sub>2</sub>	0.688 <sub>7</sub>	0.844 <sub>6</sub>	0.531 <sub>9</sub>	0.875 <sub>4</sub>	0.625 <sub>8</sub>	0.906 <sub>2</sub>	<b>0.938<sub>1</sub></b>
car	0.827 <sub>7</sub>	0.988 <sub>2</sub>	0.673 <sub>9</sub>	0.974 <sub>5</sub>	0.855 <sub>6</sub>	0.977 <sub>4</sub>	0.754 <sub>8</sub>	0.986 <sub>3</sub>	<b>0.991<sub>1</sub></b>
contraceptive	0.539 <sub>8</sub>	0.583 <sub>5</sub>	0.580 <sub>7</sub>	0.536 <sub>9</sub>	0.593 <sub>3</sub>	<b>0.600<sub>1</sub></b>	0.586 <sub>4</sub>	0.583 <sub>5</sub>	0.597 <sub>2</sub>
dermatology	<b>0.973<sub>1</sub></b>	0.946 <sub>5</sub>	0.297 <sub>9</sub>	0.932 <sub>7</sub>	0.797 <sub>8</sub>	<b>0.973<sub>1</sub></b>	0.959 <sub>4</sub>	0.946 <sub>5</sub>	0.972 <sub>3</sub>
ecoli2	0.926 <sub>5</sub>	0.882 <sub>8</sub>	0.941 <sub>4</sub>	0.897 <sub>7</sub>	0.956 <sub>2</sub>	0.809 <sub>9</sub>	<b>0.971<sub>1</sub></b>	0.912 <sub>6</sub>	0.956 <sub>2</sub>
glass	0.605 <sub>7</sub>	0.698 <sub>4</sub>	0.395 <sub>9</sub>	0.744 <sub>2</sub>	0.651 <sub>6</sub>	0.674 <sub>5</sub>	0.512 <sub>8</sub>	0.721 <sub>3</sub>	<b>0.814<sub>1</sub></b>
haberman	0.677 <sub>5</sub>	0.710 <sub>3</sub>	0.629 <sub>9</sub>	0.677 <sub>5</sub>	0.694 <sub>4</sub>	0.645 <sub>8</sub>	0.661 <sub>7</sub>	0.742 <sub>1</sub>	<b>0.742<sub>1</sub></b>
hayesroth	0.963 <sub>2</sub>	<b>1.000<sub>1</sub></b>	0.778 <sub>7</sub>	0.889 <sub>6</sub>	0.630 <sub>8</sub>	0.926 <sub>3</sub>	0.630 <sub>8</sub>	0.926 <sub>3</sub>	0.926 <sub>3</sub>
heart	0.796 <sub>3</sub>	0.759 <sub>7</sub>	0.815 <sub>2</sub>	0.648 <sub>9</sub>	<b>0.833<sub>1</sub></b>	0.778 <sub>5</sub>	0.759 <sub>7</sub>	0.778 <sub>5</sub>	0.796 <sub>3</sub>
led7digit	0.630 <sub>8</sub>	0.550 <sub>9</sub>	0.730 <sub>1</sub>	0.690 <sub>5</sub>	0.710 <sub>3</sub>	0.680 <sub>7</sub>	0.690 <sub>5</sub>	0.700 <sub>4</sub>	<b>0.730<sub>1</sub></b>
newthyroid	0.907 <sub>8</sub>	0.930 <sub>7</sub>	0.977 <sub>2</sub>	0.884 <sub>9</sub>	0.977 <sub>2</sub>	0.953 <sub>5</sub>	0.953 <sub>5</sub>	0.977 <sub>2</sub>	<b>1.000<sub>1</sub></b>
newthyroid1	0.930 <sub>7</sub>	0.930 <sub>7</sub>	1.000 <sub>1</sub>	0.930 <sub>7</sub>	1.000 <sub>1</sub>	0.977 <sub>5</sub>	1.000 <sub>1</sub>	0.977 <sub>5</sub>	<b>1.000<sub>1</sub></b>
newthyroid2	<b>1.000<sub>1</sub></b>	0.953 <sub>7</sub>	<b>1.000<sub>1</sub></b>	0.953 <sub>7</sub>	0.977 <sub>4</sub>	0.953 <sub>7</sub>	<b>1.000<sub>1</sub></b>	0.977 <sub>4</sub>	0.977 <sub>4</sub>
pageblocks	0.844 <sub>8</sub>	0.954 <sub>5</sub>	0.716 <sub>9</sub>	0.963 <sub>4</sub>	0.945 <sub>7</sub>	0.972 <sub>2</sub>	0.954 <sub>5</sub>	0.972 <sub>2</sub>	<b>0.982<sub>1</sub></b>
shuttle	0.713 <sub>7</sub>	0.998 <sub>4</sub>	0.159 <sub>9</sub>	0.998 <sub>4</sub>	1.000 <sub>1</sub>	0.998 <sub>4</sub>	0.710 <sub>8</sub>	1.000 <sub>1</sub>	<b>1.000<sub>1</sub></b>
tae	0.581 <sub>6</sub>	0.613 <sub>4</sub>	0.613 <sub>4</sub>	<b>0.677<sub>1</sub></b>	0.581 <sub>6</sub>	<b>0.677<sub>1</sub></b>	0.548 <sub>8</sub>	0.548 <sub>8</sub>	0.645 <sub>3</sub>
thyroid	0.979 <sub>1</sub>	0.979 <sub>1</sub>	0.979 <sub>1</sub>	0.972 <sub>6</sub>	0.972 <sub>6</sub>	0.972 <sub>6</sub>	0.979 <sub>1</sub>	0.958 <sub>9</sub>	<b>0.979<sub>1</sub></b>
vehicle	0.747 <sub>3</sub>	0.741 <sub>5</sub>	0.618 <sub>8</sub>	0.741 <sub>5</sub>	0.647 <sub>7</sub>	0.753 <sub>2</sub>	0.553 <sub>9</sub>	0.747 <sub>3</sub>	<b>0.818<sub>1</sub></b>
wine	0.972 <sub>4</sub>	0.861 <sub>8</sub>	1.000 <sub>1</sub>	0.861 <sub>8</sub>	1.000 <sub>1</sub>	0.972 <sub>4</sub>	0.972 <sub>4</sub>	0.972 <sub>4</sub>	<b>1.000<sub>1</sub></b>
zoo	0.952 <sub>3</sub>	0.952 <sub>3</sub>	0.857 <sub>7</sub>	0.952 <sub>3</sub>	0.810 <sub>8</sub>	0.952 <sub>3</sub>	0.762 <sub>9</sub>	1.000 <sub>1</sub>	<b>1.000<sub>1</sub></b>

Table 6: Comparison of Weighted F1-score and Rank.

Dataset	AdaBoostAD	AdaBoostNC	GBSMOTE	LexiBoost	MCNRO	MultiRandBal	NROMM	OREMBoost	Ours
automobile	0.874 <sub>4</sub>	0.906 <sub>2</sub>	0.720 <sub>7</sub>	0.841 <sub>6</sub>	0.515 <sub>9</sub>	0.874 <sub>4</sub>	0.624 <sub>8</sub>	0.897 <sub>3</sub>	<b>0.937<sub>1</sub></b>
car	0.842 <sub>6</sub>	0.988 <sub>2</sub>	0.715 <sub>9</sub>	0.974 <sub>5</sub>	0.829 <sub>7</sub>	0.977 <sub>4</sub>	0.789 <sub>8</sub>	0.986 <sub>3</sub>	<b>0.991<sub>1</sub></b>
contraceptive	0.534 <sub>9</sub>	0.585 <sub>7</sub>	0.590 <sub>4</sub>	0.535 <sub>8</sub>	0.590 <sub>4</sub>	<b>0.603<sub>1</sub></b>	0.587 <sub>6</sub>	0.591 <sub>3</sub>	0.597 <sub>2</sub>
dermatology	<b>0.973<sub>1</sub></b>	0.946 <sub>5</sub>	0.186 <sub>9</sub>	0.933 <sub>7</sub>	0.798 <sub>8</sub>	<b>0.973<sub>1</sub></b>	0.960 <sub>4</sub>	0.947 <sub>5</sub>	0.972 <sub>3</sub>
ecoli2	0.928 <sub>5</sub>	0.877 <sub>8</sub>	0.941 <sub>4</sub>	0.899 <sub>7</sub>	0.955 <sub>2</sub>	0.830 <sub>9</sub>	<b>0.971<sub>1</sub></b>	0.915 <sub>6</sub>	0.955 <sub>2</sub>
glass	0.623 <sub>6</sub>	0.698 <sub>4</sub>	0.382 <sub>9</sub>	0.747 <sub>2</sub>	0.607 <sub>7</sub>	0.674 <sub>5</sub>	0.519 <sub>8</sub>	0.725 <sub>3</sub>	<b>0.808<sub>1</sub></b>
haberman	0.692 <sub>5</sub>	0.710 <sub>3</sub>	0.652 <sub>9</sub>	0.688 <sub>6</sub>	0.702 <sub>4</sub>	0.664 <sub>8</sub>	0.682 <sub>7</sub>	0.742 <sub>2</sub>	<b>0.750<sub>1</sub></b>
hayesroth	0.963 <sub>2</sub>	<b>1.000<sub>1</sub></b>	0.780 <sub>7</sub>	0.889 <sub>6</sub>	0.502 <sub>9</sub>	0.926 <sub>3</sub>	0.556 <sub>8</sub>	0.926 <sub>3</sub>	0.926 <sub>3</sub>
heart	0.809 <sub>4</sub>	0.769 <sub>8</sub>	0.828 <sub>2</sub>	0.682 <sub>9</sub>	<b>0.836<sub>1</sub></b>	0.793 <sub>5</sub>	0.782 <sub>7</sub>	0.793 <sub>5</sub>	0.812 <sub>3</sub>
led7digit	0.617 <sub>8</sub>	0.527 <sub>9</sub>	<b>0.735<sub>1</sub></b>	0.691 <sub>6</sub>	0.703 <sub>4</sub>	0.684 <sub>7</sub>	0.693 <sub>5</sub>	0.705 <sub>3</sub>	0.731 <sub>2</sub>
newthyroid	0.909 <sub>8</sub>	0.927 <sub>7</sub>	0.976 <sub>2</sub>	0.884 <sub>9</sub>	0.976 <sub>2</sub>	0.952 <sub>5</sub>	0.950 <sub>6</sub>	0.976 <sub>2</sub>	<b>1.000<sub>1</sub></b>
newthyroid1	0.935 <sub>7</sub>	0.935 <sub>7</sub>	1.000 <sub>1</sub>	0.935 <sub>7</sub>	1.000 <sub>1</sub>	0.977 <sub>5</sub>	1.000 <sub>1</sub>	0.977 <sub>5</sub>	<b>1.000<sub>1</sub></b>
newthyroid2	<b>1.000<sub>1</sub></b>	0.950 <sub>7</sub>	<b>1.000<sub>1</sub></b>	0.950 <sub>7</sub>	0.976 <sub>4</sub>	0.950 <sub>7</sub>	<b>1.000<sub>1</sub></b>	0.976 <sub>4</sub>	0.976 <sub>4</sub>
pageblocks	0.883 <sub>8</sub>	0.953 <sub>6</sub>	0.787 <sub>9</sub>	0.961 <sub>4</sub>	0.930 <sub>7</sub>	0.973 <sub>3</sub>	0.956 <sub>5</sub>	0.974 <sub>2</sub>	<b>0.981<sub>1</sub></b>
shuttle	0.823 <sub>7</sub>	0.997 <sub>5</sub>	0.044 <sub>9</sub>	0.997 <sub>5</sub>	1.000 <sub>1</sub>	0.998 <sub>4</sub>	0.747 <sub>8</sub>	1.000 <sub>1</sub>	<b>1.000<sub>1</sub></b>
tae	0.578 <sub>7</sub>	0.606 <sub>5</sub>	0.608 <sub>4</sub>	<b>0.679<sub>1</sub></b>	0.580 <sub>6</sub>	0.678 <sub>2</sub>	0.528 <sub>9</sub>	0.554 <sub>8</sub>	0.646 <sub>3</sub>
thyroid	0.981 <sub>1</sub>	0.979 <sub>5</sub>	0.981 <sub>1</sub>	0.973 <sub>7</sub>	0.973 <sub>7</sub>	0.974 <sub>6</sub>	0.981 <sub>1</sub>	0.957 <sub>9</sub>	<b>0.981<sub>1</sub></b>
vehicle	0.747 <sub>2</sub>	0.736 <sub>6</sub>	0.607 <sub>8</sub>	0.737 <sub>5</sub>	0.630 <sub>7</sub>	0.739 <sub>4</sub>	0.531 <sub>9</sub>	0.742 <sub>3</sub>	<b>0.810<sub>1</sub></b>
wine	0.972 <sub>4</sub>	0.859 <sub>9</sub>	1.000 <sub>1</sub>	0.863 <sub>8</sub>	1.000 <sub>1</sub>	0.972 <sub>4</sub>	0.972 <sub>4</sub>	0.972 <sub>4</sub>	<b>1.000<sub>1</sub></b>
zoo	0.949 <sub>3</sub>	0.949 <sub>3</sub>	0.810 <sub>7</sub>	0.949 <sub>3</sub>	0.764 <sub>8</sub>	0.949 <sub>3</sub>	0.743 <sub>9</sub>	1.000 <sub>1</sub>	<b>1.000<sub>1</sub></b>

#### 4.5 Ablation Analysis

To evaluate the contribution of each core component quantitatively, we conducted ablation studies across five configurations. We assessed the Density Factor (DF), Confidence Factor (CF), and Region-Guided Generation (RG). Table 10 summarizes these results. The bolded values represent the best performance.

The DF provides effective geometric noise constraints. Using the DF alone generally improves performance by quantifying local density and suppressing isolated noise. However, relying solely on density can lead to indiscriminate suppression. While it filters noise, it may also discard valuable boundary samples in low-density regions, which limits performance gains on specific datasets.

Similarly, relying solely on the CF can lead to overfitting on noise, sometimes degrading performance below the baseline. For instance, on the automobile dataset, accuracy dropped from the baseline of 0.844 to 0.688. Much like traditional AdaBoost, difficulty-based weighting often misidentifies noise in overlapping regions as hard samples. Without density constraints, the model overemphasizes these noise points, distorting decision boundaries and impairing generalization.

Table 7: Comparison of G-Mean and Rank.

Dataset	AdaBoostAD	AdaBoostNC	GBSMOTE	LexiBoost	MCNRO	MultiRandBal	NROMM	OREMBoost	Ours
automobile	0.866 <sub>3</sub>	0.891 <sub>2</sub>	0.699 <sub>7</sub>	0.852 <sub>5</sub>	0.600 <sub>9</sub>	0.866 <sub>3</sub>	0.616 <sub>8</sub>	0.803 <sub>6</sub>	<b>0.910<sub>1</sub></b>
car	0.894 <sub>7</sub>	0.958 <sub>4</sub>	0.690 <sub>9</sub>	0.949 <sub>5</sub>	0.912 <sub>6</sub>	0.985 <sub>3</sub>	0.825 <sub>8</sub>	0.990 <sub>2</sub>	<b>0.992<sub>1</sub></b>
contraceptive	0.492 <sub>9</sub>	0.557 <sub>6</sub>	0.572 <sub>3</sub>	0.510 <sub>8</sub>	0.550 <sub>7</sub>	<b>0.586<sub>1</sub></b>	0.563 <sub>5</sub>	0.578 <sub>2</sub>	0.572 <sub>3</sub>
dermatology	0.970 <sub>3</sub>	0.941 <sub>7</sub>	<b>1.000<sub>1</sub></b>	0.918 <sub>8</sub>	0.697 <sub>9</sub>	0.978 <sub>2</sub>	0.967 <sub>4</sub>	0.950 <sub>6</sub>	0.963 <sub>5</sub>
ecoli2	0.880 <sub>5</sub>	0.719 <sub>9</sub>	0.889 <sub>4</sub>	0.822 <sub>8</sub>	0.897 <sub>2</sub>	0.847 <sub>7</sub>	<b>0.945<sub>1</sub></b>	0.872 <sub>6</sub>	0.897 <sub>2</sub>
glass	0.709 <sub>6</sub>	0.701 <sub>7</sub>	0.383 <sub>9</sub>	0.725 <sub>4</sub>	0.749 <sub>3</sub>	<b>0.814<sub>1</sub></b>	0.563 <sub>8</sub>	0.713 <sub>5</sub>	0.758 <sub>2</sub>
haberman	0.635 <sub>5</sub>	0.593 <sub>9</sub>	0.647 <sub>3</sub>	0.608 <sub>8</sub>	0.617 <sub>6</sub>	0.616 <sub>7</sub>	0.670 <sub>2</sub>	0.643 <sub>4</sub>	<b>0.699<sub>1</sub></b>
hayesroth	0.969 <sub>3</sub>	<b>1.000<sub>1</sub></b>	0.781 <sub>8</sub>	0.903 <sub>7</sub>	<b>1.000<sub>1</sub></b>	0.935 <sub>4</sub>	0.450 <sub>9</sub>	0.935 <sub>4</sub>	0.935 <sub>4</sub>
heart	0.769 <sub>4</sub>	0.666 <sub>9</sub>	<b>0.816<sub>1</sub></b>	0.676 <sub>8</sub>	0.750 <sub>7</sub>	0.758 <sub>5</sub>	0.810 <sub>2</sub>	0.758 <sub>5</sub>	0.804 <sub>3</sub>
led7digit	0.563 <sub>8</sub>	0.445 <sub>9</sub>	<b>0.728<sub>1</sub></b>	0.664 <sub>5</sub>	0.630 <sub>7</sub>	0.656 <sub>6</sub>	0.673 <sub>4</sub>	0.684 <sub>3</sub>	0.716 <sub>2</sub>
newthyroid	0.909 <sub>5</sub>	0.841 <sub>9</sub>	0.941 <sub>3</sub>	0.843 <sub>8</sub>	0.941 <sub>3</sub>	0.894 <sub>6</sub>	0.874 <sub>7</sub>	0.950 <sub>2</sub>	<b>1.000<sub>1</sub></b>
newthyroid1	0.957 <sub>7</sub>	0.957 <sub>7</sub>	1.000 <sub>1</sub>	0.957 <sub>7</sub>	1.000 <sub>1</sub>	0.986 <sub>5</sub>	1.000 <sub>1</sub>	0.986 <sub>5</sub>	<b>1.000<sub>1</sub></b>
newthyroid2	<b>1.000<sub>1</sub></b>	0.845 <sub>7</sub>	<b>1.000<sub>1</sub></b>	0.845 <sub>7</sub>	0.926 <sub>4</sub>	0.845 <sub>7</sub>	<b>1.000<sub>1</sub></b>	0.926 <sub>4</sub>	0.926 <sub>4</sub>
pageblocks	0.882 <sub>4</sub>	0.865 <sub>6</sub>	0.675 <sub>9</sub>	0.867 <sub>5</sub>	0.754 <sub>8</sub>	0.917 <sub>2</sub>	0.769 <sub>7</sub>	0.917 <sub>2</sub>	<b>0.919<sub>1</sub></b>
shuttle	0.801 <sub>9</sub>	1.000 <sub>1</sub>	1.000 <sub>1</sub>	1.000 <sub>1</sub>	1.000 <sub>1</sub>	0.999 <sub>7</sub>	0.891 <sub>8</sub>	1.000 <sub>1</sub>	<b>1.000<sub>1</sub></b>
tae	0.576 <sub>6</sub>	0.602 <sub>4</sub>	0.602 <sub>4</sub>	0.673 <sub>2</sub>	0.576 <sub>6</sub>	<b>0.678<sub>1</sub></b>	0.511 <sub>9</sub>	0.547 <sub>8</sub>	0.634 <sub>3</sub>
thyroid	0.992 <sub>1</sub>	0.869 <sub>7</sub>	0.992 <sub>1</sub>	0.867 <sub>8</sub>	0.949 <sub>6</sub>	0.990 <sub>5</sub>	0.992 <sub>1</sub>	0.686 <sub>9</sub>	<b>0.992<sub>1</sub></b>
vehicle	0.732 <sub>2</sub>	0.721 <sub>5</sub>	0.580 <sub>8</sub>	0.723 <sub>4</sub>	0.609 <sub>7</sub>	0.717 <sub>6</sub>	0.513 <sub>9</sub>	0.728 <sub>3</sub>	<b>0.798<sub>1</sub></b>
wine	0.976 <sub>4</sub>	0.863 <sub>8</sub>	1.000 <sub>1</sub>	0.863 <sub>8</sub>	1.000 <sub>1</sub>	0.976 <sub>4</sub>	0.976 <sub>4</sub>	0.976 <sub>4</sub>	<b>1.000<sub>1</sub></b>
zoo	0.906 <sub>5</sub>	0.906 <sub>5</sub>	1.000 <sub>1</sub>	0.906 <sub>5</sub>	0.974 <sub>4</sub>	0.906 <sub>5</sub>	0.871 <sub>9</sub>	1.000 <sub>1</sub>	<b>1.000<sub>1</sub></b>

Table 8: Comparison of AUC and Rank.

Dataset	AdaBoostAD	AdaBoostNC	GBSMOTE	LexiBoost	MCNRO	MultiRandBal	NROMM	OREMBoost	Ours
automobile	0.914 <sub>5</sub>	0.945 <sub>4</sub>	0.886 <sub>7</sub>	0.910 <sub>6</sub>	0.842 <sub>9</sub>	0.952 <sub>3</sub>	0.877 <sub>8</sub>	0.960 <sub>2</sub>	<b>0.966<sub>1</sub></b>
car	0.977 <sub>5</sub>	0.999 <sub>1</sub>	0.831 <sub>9</sub>	0.968 <sub>6</sub>	0.934 <sub>7</sub>	0.999 <sub>1</sub>	0.924 <sub>8</sub>	0.992 <sub>4</sub>	<b>0.999<sub>1</sub></b>
contraceptive	0.703 <sub>9</sub>	0.726 <sub>6</sub>	0.732 <sub>5</sub>	0.720 <sub>7</sub>	0.744 <sub>3</sub>	<b>0.768<sub>1</sub></b>	0.741 <sub>4</sub>	0.756 <sub>2</sub>	0.707 <sub>8</sub>
dermatology	0.996 <sub>3</sub>	0.965 <sub>7</sub>	0.786 <sub>9</sub>	0.975 <sub>5</sub>	0.949 <sub>8</sub>	0.998 <sub>2</sub>	0.984 <sub>4</sub>	0.970 <sub>6</sub>	<b>0.999<sub>1</sub></b>
ecoli2	0.951 <sub>4</sub>	0.746 <sub>9</sub>	<b>0.992<sub>1</sub></b>	0.894 <sub>7</sub>	0.986 <sub>2</sub>	0.905 <sub>5</sub>	0.978 <sub>3</sub>	0.876 <sub>8</sub>	0.901 <sub>6</sub>
glass	0.912 <sub>3</sub>	0.840 <sub>9</sub>	0.875 <sub>7</sub>	0.856 <sub>8</sub>	0.881 <sub>6</sub>	0.928 <sub>2</sub>	0.882 <sub>5</sub>	0.885 <sub>4</sub>	<b>0.946<sub>1</sub></b>
haberman	<b>0.704<sub>1</sub></b>	0.631 <sub>8</sub>	0.636 <sub>7</sub>	0.613 <sub>9</sub>	0.640 <sub>6</sub>	0.685 <sub>4</sub>	0.661 <sub>5</sub>	0.696 <sub>3</sub>	0.700 <sub>2</sub>
hayesroth	0.996 <sub>2</sub>	<b>1.000<sub>1</sub></b>	0.927 <sub>7</sub>	0.992 <sub>4</sub>	0.788 <sub>9</sub>	0.992 <sub>4</sub>	0.863 <sub>8</sub>	0.992 <sub>4</sub>	0.996 <sub>2</sub>
heart	0.762 <sub>6</sub>	0.733 <sub>8</sub>	<b>0.875<sub>1</sub></b>	0.678 <sub>9</sub>	0.829 <sub>4</sub>	0.830 <sub>3</sub>	0.852 <sub>2</sub>	0.751 <sub>7</sub>	0.796 <sub>5</sub>
led7digit	0.864 <sub>7</sub>	0.852 <sub>9</sub>	0.936 <sub>2</sub>	0.886 <sub>6</sub>	<b>0.941<sub>1</sub></b>	0.934 <sub>3</sub>	0.929 <sub>4</sub>	0.853 <sub>8</sub>	0.927 <sub>5</sub>
newthyroid	0.969 <sub>6</sub>	0.886 <sub>9</sub>	0.993 <sub>4</sub>	0.898 <sub>7</sub>	0.994 <sub>3</sub>	0.998 <sub>2</sub>	0.895 <sub>8</sub>	0.987 <sub>5</sub>	<b>1.000<sub>1</sub></b>
newthyroid1	0.986 <sub>6</sub>	0.958 <sub>8</sub>	1.000 <sub>1</sub>	0.958 <sub>8</sub>	1.000 <sub>1</sub>	1.000 <sub>1</sub>	1.000 <sub>1</sub>	0.986 <sub>6</sub>	<b>1.000<sub>1</sub></b>
newthyroid2	<b>1.000<sub>1</sub></b>	0.857 <sub>8</sub>	<b>1.000<sub>1</sub></b>	0.857 <sub>8</sub>	<b>1.000<sub>1</sub></b>	0.998 <sub>5</sub>	<b>1.000<sub>1</sub></b>	0.929 <sub>6</sub>	0.927 <sub>7</sub>
pageblocks	0.911 <sub>7</sub>	0.918 <sub>6</sub>	0.757 <sub>9</sub>	0.920 <sub>5</sub>	0.927 <sub>3</sub>	0.925 <sub>4</sub>	0.889 <sub>8</sub>	<b>0.949<sub>1</sub></b>	0.946 <sub>2</sub>
shuttle	0.934 <sub>6</sub>	0.875 <sub>7</sub>	0.785 <sub>9</sub>	0.875 <sub>7</sub>	1.000 <sub>1</sub>	0.999 <sub>4</sub>	0.999 <sub>4</sub>	1.000 <sub>1</sub>	<b>1.000<sub>1</sub></b>
tae	0.772 <sub>5</sub>	0.774 <sub>3</sub>	0.774 <sub>3</sub>	0.766 <sub>6</sub>	0.745 <sub>7</sub>	0.778 <sub>2</sub>	0.674 <sub>9</sub>	0.708 <sub>8</sub>	<b>0.792<sub>1</sub></b>
thyroid	0.995 <sub>2</sub>	0.924 <sub>7</sub>	0.994 <sub>3</sub>	0.922 <sub>8</sub>	0.994 <sub>3</sub>	<b>0.997<sub>1</sub></b>	0.994 <sub>3</sub>	0.849 <sub>9</sub>	0.989 <sub>6</sub>
vehicle	0.910 <sub>3</sub>	0.828 <sub>7</sub>	0.845 <sub>6</sub>	0.828 <sub>7</sub>	0.851 <sub>5</sub>	0.927 <sub>2</sub>	0.770 <sub>9</sub>	0.853 <sub>4</sub>	<b>0.942<sub>1</sub></b>
wine	0.993 <sub>5</sub>	0.898 <sub>9</sub>	0.999 <sub>4</sub>	0.902 <sub>8</sub>	1.000 <sub>1</sub>	1.000 <sub>1</sub>	0.985 <sub>7</sub>	0.993 <sub>5</sub>	<b>1.000<sub>1</sub></b>
zoo	0.957 <sub>9</sub>	0.961 <sub>7</sub>	0.964 <sub>6</sub>	0.961 <sub>7</sub>	0.985 <sub>4</sub>	1.000 <sub>1</sub>	0.985 <sub>4</sub>	1.000 <sub>1</sub>	<b>1.000<sub>1</sub></b>

Table 9: Average Rank of Different Metrics.

Metric	AdaBoostAD	AdaBoostNC	GBSMOTE	LexiBoost	MCNRO	MultiRandBal	NROMM	OREMBoost	Ours
Accuracy	4.88	5.19	4.69	5.50	4.19	4.75	5.44	3.81	<b>1.62</b>
Weighted F1	4.88	5.81	4.69	5.75	4.44	5.00	5.56	3.81	<b>1.69</b>
G-Mean	4.69	6.44	3.50	5.94	4.19	4.88	5.12	4.12	<b>1.81</b>
AUC	4.56	7.19	4.44	7.12	3.56	2.75	5.06	5.00	<b>2.69</b>

Combining the DF and CF creates a synergistic effect. The DF suppresses isolated outliers using geometric information, while the CF targets boundary samples. This combination allows the model to distinguish between noise and legitimate hard samples, a task that traditional Boosting generally difficult to achieve.

Incorporating the RG strategy yields the best performance on 17 datasets. This suggests that weight adjustment alone is not enough to give full play to address severe class skew and overlap. The RG strategy leverages partitioned regions to establish a boundary-to-dense generation path. By pulling ambiguous boundary samples toward dense regions, this strategy balances the class distribution and reconstructs clear decision boundaries. This process achieves a closed-loop cooperative optimization between imbalanced learning and Boosting.

In summary, the proposed model tightly couples sample weight updates with dynamic sampling. This cooperative optimization delivers robust and superior recognition performance in complex multiclass imbalanced tasks.

Table 10: Ablation study results. DF: Density Factor, CF: Confidence Factor, RG: Region-Guided.

Dataset	Components			Metrics				Dataset	Components			Metrics			
	DF	CF	RG	Acc	F1	GM	AUC		DF	CF	RG	Acc	F1	GM	AUC
automobile	×	×	×	0.844	0.843	0.839	<b>0.969</b>	newthyroid	×	×	×	0.953	0.950	0.894	0.922
	✓	×	×	0.906	0.906	0.839	0.965		✓	×	×	0.930	0.928	0.884	0.955
	×	✓	×	0.688	0.651	0.716	0.916		×	✓	×	0.953	0.950	0.894	0.922
	✓	✓	×	0.906	0.903	0.839	0.959		✓	✓	×	0.953	0.950	0.894	0.922
	✓	✓	✓	<b>0.938</b>	<b>0.937</b>	<b>0.910</b>	0.966		✓	✓	✓	<b>1.000</b>	<b>1.000</b>	<b>1.000</b>	<b>1.000</b>
car	×	×	×	0.986	0.986	0.988	0.999	newthyroid1	×	×	×	1.000	1.000	1.000	1.000
	✓	×	×	0.986	0.986	0.973	<b>1.000</b>		✓	×	×	0.907	0.915	0.943	1.000
	×	✓	×	0.977	0.976	0.928	0.999		×	✓	×	0.953	0.956	0.972	1.000
	✓	✓	×	0.983	0.983	0.987	0.999		✓	✓	×	0.907	0.915	0.943	1.000
	✓	✓	✓	<b>0.991</b>	<b>0.991</b>	<b>0.992</b>	0.999		✓	✓	✓	<b>1.000</b>	<b>1.000</b>	<b>1.000</b>	<b>1.000</b>
contraceptive	×	×	×	0.529	0.528	0.502	<b>0.714</b>	newthyroid2	×	×	×	0.953	0.950	0.845	0.857
	✓	×	×	0.427	0.384	0.343	0.703		✓	×	×	0.953	0.950	0.845	0.857
	×	✓	×	0.569	0.567	0.529	0.660		×	✓	×	0.953	0.950	0.845	0.857
	✓	✓	×	<b>0.593</b>	<b>0.588</b>	0.543	0.706		✓	✓	×	0.953	0.950	0.845	0.857
	✓	✓	✓	0.583	0.580	<b>0.546</b>	0.707		✓	✓	✓	<b>0.977</b>	<b>0.976</b>	<b>0.926</b>	<b>0.927</b>
dermatology	×	×	×	0.932	0.934	0.926	0.994	pageblocks	×	×	×	0.963	0.964	0.915	0.946
	✓	×	×	0.959	0.959	0.953	0.996		✓	×	×	0.963	0.961	0.867	0.946
	×	✓	×	0.865	0.848	0.780	0.993		×	✓	×	0.963	0.964	0.915	0.946
	✓	✓	×	0.959	0.960	0.957	0.994		✓	✓	×	0.972	0.973	0.917	0.946
	✓	✓	✓	<b>0.959</b>	<b>0.960</b>	<b>0.957</b>	<b>0.997</b>		✓	✓	✓	<b>0.982</b>	<b>0.981</b>	<b>0.919</b>	<b>0.946</b>
ecoli2	×	×	×	0.897	0.895	0.776	0.793	shuttle	×	×	×	0.998	0.997	1.000	1.000
	✓	×	×	0.897	0.899	0.822	0.875		✓	×	×	0.998	0.997	1.000	1.000
	×	✓	×	0.897	0.895	0.776	0.793		×	✓	×	0.998	0.997	1.000	1.000
	✓	✓	×	0.897	0.895	0.776	0.793		✓	✓	×	0.998	0.997	1.000	1.000
	✓	✓	✓	<b>0.956</b>	<b>0.955</b>	<b>0.897</b>	<b>0.901</b>		✓	✓	✓	<b>1.000</b>	<b>1.000</b>	<b>1.000</b>	<b>1.000</b>
glass	×	×	×	0.698	0.694	<b>0.830</b>	0.932	tae	×	×	×	0.581	0.582	0.576	0.770
	✓	×	×	0.767	0.739	0.823	0.937		✓	×	×	0.581	0.579	0.576	0.796
	×	✓	×	0.791	0.785	0.708	<b>0.953</b>		×	✓	×	<b>0.710</b>	<b>0.707</b>	<b>0.700</b>	<b>0.824</b>
	✓	✓	×	0.698	0.690	0.781	0.937		✓	✓	×	0.645	0.646	0.634	0.792
	✓	✓	✓	<b>0.814</b>	<b>0.808</b>	0.758	0.946		✓	✓	✓	0.645	0.646	0.634	0.792
haberman	×	×	×	0.694	0.690	0.549	0.639	thyroid	×	×	×	0.972	0.973	0.949	<b>0.993</b>
	✓	×	×	0.661	0.670	0.569	0.664		✓	×	×	0.958	0.959	0.788	0.986
	×	✓	×	0.694	0.697	0.585	0.582		×	✓	×	0.972	0.973	0.867	0.989
	✓	✓	×	0.710	0.715	0.626	0.664		✓	✓	×	0.958	0.959	0.788	0.984
	✓	✓	✓	<b>0.742</b>	<b>0.750</b>	<b>0.699</b>	<b>0.700</b>		✓	✓	✓	<b>0.979</b>	<b>0.981</b>	<b>0.992</b>	0.989
hayesroth	×	×	×	0.926	0.926	0.935	0.991	vehicle	×	×	×	0.753	0.746	0.724	0.930
	✓	×	×	0.778	0.771	0.717	0.989		✓	×	×	0.741	0.731	0.703	0.918
	×	✓	×	0.926	0.926	0.935	0.996		×	✓	×	0.747	0.737	0.714	0.940
	✓	✓	×	0.926	0.926	0.935	0.996		✓	✓	×	0.818	0.810	0.798	0.942
	✓	✓	✓	<b>0.926</b>	<b>0.926</b>	<b>0.935</b>	<b>0.996</b>		✓	✓	✓	<b>0.818</b>	<b>0.810</b>	<b>0.798</b>	<b>0.942</b>
heart	×	×	×	0.778	0.784	0.676	0.685	wine	×	×	×	1.000	1.000	1.000	1.000
	✓	×	×	0.796	0.793	0.634	0.722		✓	×	×	0.972	0.972	0.971	1.000
	×	✓	×	0.778	0.784	0.676	0.685		×	✓	×	0.972	0.972	0.976	0.994
	✓	✓	×	0.778	0.784	0.676	0.685		✓	✓	×	1.000	1.000	1.000	1.000
	✓	✓	✓	<b>0.796</b>	<b>0.812</b>	<b>0.804</b>	<b>0.796</b>		✓	✓	✓	<b>1.000</b>	<b>1.000</b>	<b>1.000</b>	<b>1.000</b>
led7digit	×	×	×	<b>0.740</b>	<b>0.740</b>	<b>0.724</b>	<b>0.944</b>	zoo	×	×	×	0.952	0.949	0.906	0.990
	✓	×	×	0.730	0.733	0.723	0.933		✓	×	×	0.952	0.952	0.906	1.000
	×	✓	×	0.710	0.710	0.699	0.901		×	✓	×	0.952	0.949	0.906	0.997
	✓	✓	×	0.730	0.731	0.716	0.925		✓	✓	×	0.952	0.949	0.906	0.997
	✓	✓	✓	0.730	0.731	0.716	0.927		✓	✓	✓	<b>1.000</b>	<b>1.000</b>	<b>1.000</b>	<b>1.000</b>

## 5 Conclusion

This study addresses a critical limitation in current research where imbalanced learning and model training are typically decoupled. We propose a novel collaborative optimization model: the Density-Aware and Region-Guided Boosting. Unlike traditional methods that treat data sampling and weight updates as isolated steps, we integrate these processes to establish a closed-loop synergy between imbalanced learning and ensemble construction.

Our primary contribution is the use of density factor and confidence factor as a bridge to link sample weight updates with dynamic sampling. This facilitates a unified training loop, the effectiveness of which is verified on multiple

public imbalanced datasets. This research offers a promising perspective for future developments in the field. While we achieved strong performance using AdaBoost, this collaborative optimization strategy can be extended to other ensemble models. Such an extension would yield more flexible and adaptive unified models that are highly valuable for practical applications.

However, the proposed method still has limitations. Density estimation based on nearest neighbors is only an approximation and becomes computationally expensive as the dataset size increases. Furthermore, some models do not update sample weights based solely on classification error rates; for example, the GBDTs employ residual updates. Therefore, our future work will focus on two directions. First, we will investigate simpler and more accurate region partitioning mechanisms to reduce the impact of noise and class overlap. Second, we aim to extend our collaborative optimization strategy to the GBDTs and neural networks to enable broader practical applications.

## References

- [1] A. K. Sharma and N. K. Verma. A novel vision transformer with selective residual in multihead self-attention for pattern recognition. *Pattern Recognition*, 172:112497, 2026. doi:10.1016/j.patcog.2025.112497.
- [2] X. Han, M. Lei, and J. Li. Hypergraph-based semantic and topological self-supervised learning for brain disease diagnosis. *Pattern Recognition*, 169:111921, 2026. doi:10.1016/j.patcog.2025.111921.
- [3] Z. Ding, G. Zhong, X. Qin, Q. Li, Z. Fan, Z. Deng, X. Ling, and W. Xiang. MF-Net: Multi-frequency intrusion detection network for internet traffic data. *Pattern Recognition*, 146:109999, 2024. doi:10.1016/j.patcog.2023.109999.
- [4] X. Yang, J. Ge, H. Li, L. Li, and B. Wu. ReID: Re-ranking through image description for object re-identification. *Pattern Recognition*, 172:112552, 2026. doi:10.1016/j.patcog.2025.112552.
- [5] H. Zouhri, A. Idri, and A. Ratnani. Evaluating the impact of filter-based feature selection in intrusion detection systems. *International Journal of Information Security*, 23:759–785, 2024. doi:10.1007/s10207-023-00767-y.
- [6] H. Ren, Y. Tang, S. Ren, et al. ADHS-EL: Dynamic ensemble learning with adversarial augmentation for accurate and robust network intrusion detection. *Journal of King Saud University-Computer and Information Sciences*, 37: 7, 2025. doi:10.1007/s44443-025-00015-4.
- [7] Nitesh V Chawla, Kevin W Bowyer, Lawrence O Hall, and W Philip Kegelmeyer. SMOTE: Synthetic minority over-sampling technique. *Journal of Artificial Intelligence Research*, 16(1):321–357, 2002.
- [8] Mingming Han, Husheng Guo, and Wenjian Wang. A new data complexity measure for multi-class imbalanced classification tasks. *Pattern Recognition*, 157:110881, 2025. ISSN 0031-3203. doi:10.1016/j.patcog.2024.110881.
- [9] Paria Soltanzadeh, M. Reza Feizi-Derakhshi, and Mahdi Hashemzadeh. Addressing the class-imbalance and class-overlap problems by a metaheuristic-based under-sampling approach. *Pattern Recognition*, 143:109721, 2023. ISSN 0031-3203. doi:10.1016/j.patcog.2023.109721.
- [10] Haibo He, Yang Bai, Edwardo A Garcia, and Shutao Li. ADASYN: Adaptive synthetic sampling approach for imbalanced learning. In *2008 IEEE International Joint Conference on Neural Networks (IEEE World Congress on Computational Intelligence)*, pages 1322–1328. IEEE, 2008.
- [11] P. S. Thakur, M. Jadeja, and S. S. Chouhan. CBReT: A cluster-based resampling technique for dealing with imbalanced data in code smell prediction. *Knowledge-Based Systems*, 286:111390, 2024. doi:10.1016/j.knosys.2024.111390.
- [12] X. Xie, H. Liu, S. Zeng, L. Lin, and W. Li. A novel progressively undersampling method based on the density peaks sequence for imbalanced data. *Knowledge-Based Systems*, 213:106689, 2021. doi:10.1016/j.knosys.2020.106689.
- [13] X. Tao, A. Xu, L. Shi, J. Li, X. Guo, and S. Tao. Density clustering hypersphere-based self-adaptively oversampling algorithm for imbalanced datasets. *Knowledge-Based Systems*, 329:114407, 2025. doi:10.1016/j.knosys.2025.114407.
- [14] Z. Ren, Y. Zhu, W. Kang, H. Fu, Q. Niu, D. Gao, K. Yan, and J. Hong. Adaptive cost-sensitive learning: Improving the convergence of intelligent diagnosis models under imbalanced data. *Knowledge-Based Systems*, 241:108296, 2022. doi:10.1016/j.knosys.2022.108296.
- [15] Salman H Khan, Munawar Hayat, Mohammed Bennamoun, Ferdous A Sohel, and Roberto Togneri. Cost-sensitive learning of deep feature representations from imbalanced data. *IEEE Transactions on Neural Networks and Learning Systems*, 29(8):3573–3587, 2018. doi:10.1109/TNNLS.2017.2732482.
- [16] Juan J Rodríguez, José-Francisco Díez-Pastor, Álvar Arnaiz-González, and Ludmila I Kuncheva. Random balance ensembles for multiclass imbalance learning. *Knowledge-Based Systems*, 193:105434, 2020. doi:10.1016/j.knosys.2019.105434.

[17] T. Zhu, X. Liu, and E. Zhu. Oversampling with reliably expanding minority class regions for imbalanced data learning. *IEEE Transactions on Knowledge and Data Engineering*, 35(6):6167–6181, 2023. doi:10.1109/TKDE.2022.3171706.

[18] S. Li, L. Song, X. Wu, Z. Hu, Y. Cheung, and X. Yao. Multi-class imbalance classification based on data distribution and adaptive weights. *IEEE Transactions on Knowledge and Data Engineering*, 36(10):5265–5279, 2024. doi:10.1109/TKDE.2024.3384961.

[19] Hui Han, Wen-Yuan Wang, and Bing-Huan Mao. Borderline-SMOTE: A new over-sampling method in imbalanced data sets learning. In *Advances in Intelligent Computing*, pages 878–887. Springer, 2005. doi:10.1007/11538059\_91.

[20] Sukarna Barua, Md Monirul Islam, Xin Yao, and Kazuyuki Murase. MWMOTE—Majority weighted minority oversampling technique for imbalanced data set learning. *IEEE Transactions on Knowledge and Data Engineering*, 26(2):405–425, 2014. doi:10.1109/TKDE.2012.232.

[21] Y. Liu, Y. Liu, B. X. B. Yu, S. Zhong, and Z. Hu. Noise-robust oversampling for imbalanced data classification. *Pattern Recognition*, 133:109008, 2023. doi:10.1016/j.patcog.2022.109008.

[22] S. Shen, Z. Li, Z. Huan, F. Shang, Y. Wang, and Y. Chen. Neighborhood repartition-based oversampling algorithm for multiclass imbalanced data with label noise. *Neurocomputing*, 600:128090, 2024. doi:10.1016/j.neucom.2024.128090.

[23] T. Xia, Y. Shao, S. Xia, Y. Xiong, X. Lian, and W. Ling. GBMOTE: A robust sampling method based on granular-ball computing and smote for class imbalance. In *Proceedings of the 2023 8th International Conference on Mathematics and Artificial Intelligence*, pages 19–24. ACM, 2023. doi:10.1145/3594300.3594304.

[24] Shuo Wang and Xin Yao. Multiclass imbalance problems: Analysis and potential solutions. *IEEE Transactions on Systems, Man, and Cybernetics, Part B (Cybernetics)*, 42(4):1119–1130, 2012. doi:10.1109/TSMCB.2012.2187280.

[25] J. Tang, Y. Li, Z. Hou, S. Fu, and Y. Tian. Robust two-stage instance-level cost-sensitive learning method for class imbalance problem. *Knowledge-Based Systems*, 300:112143, 2024. doi:10.1016/j.knosys.2024.112143.

[26] Chris Seiffert, Taghi M Khoshgoftaar, Jason Van Hulse, and Amri Napolitano. RUSBoost: A hybrid approach to alleviating class imbalance. *IEEE Transactions on Systems, Man, and Cybernetics-Part A: Systems and Humans*, 40(1):185–197, 2010. doi:10.1109/TSMCA.2009.2029559.

[27] Z. Jan, J. C. Munos, and A. Ali. A novel method for creating an optimized ensemble classifier by introducing cluster size reduction and diversity. *IEEE Transactions on Knowledge and Data Engineering*, 34(7):3072–3081, 2022. doi:10.1109/TKDE.2020.3025173.

[28] Yoav Freund and Robert E Schapire. A decision-theoretic generalization of on-line learning and an application to boosting. *Journal of Computer and System Sciences*, 55(1):119–139, 1997. doi:10.1006/jcss.1997.1504.

[29] Gaetano Zazzaro. Cross-testing methodology for pattern learning and model transfer in rare fog events detection. *Pattern Recognition*, 165:111649, 2025. ISSN 0031-3203. doi:10.1016/j.patcog.2025.111649.

[30] Zeyu Teng, Peng Cao, Min Huang, Zheming Gao, and Xingwei Wang. Multi-label borderline oversampling technique. *Pattern Recognition*, 145:109953, 2024. ISSN 0031-3203. doi:10.1016/j.patcog.2023.109953.

[31] G. Schwarz. Estimating the dimension of a model. *The Annals of Statistics*, 6(2):461–464, 1978. doi:10.1214/aos/1176344136.

[32] Jesús Alcalá-Fdez, Alberto Fernández, Julián Luengo, Joaquín Derrac, Salvador García, Luciano Sánchez, and Francisco Herrera. Keel data-mining software tool: Data set repository, integration of algorithms and experimental analysis framework. *Journal of Multiple-Valued Logic and Soft Computing*, 17(2-3):255–287, 2011.

[33] Ron Kohavi. A study of cross-validation and bootstrap for accuracy estimation and model selection. In *Proceedings of the 14th International Joint Conference on Artificial Intelligence (IJCAI)*, volume 14, pages 1137–1145, 1995.

[34] Mervyn Stone. Cross-validatory choice and assessment of statistical predictions. *Journal of the Royal Statistical Society: Series B (Methodological)*, 36(2):111–133, 1974. doi:10.1111/j.2517-6161.1974.tb00994.x.

[35] Bobak Shahriari, Kevin Swersky, Ziyu Wang, Ryan P Adams, and Nando de Freitas. Taking the human out of the loop: A review of bayesian optimization. *Proceedings of the IEEE*, 104(1):148–175, 2015. doi:10.1109/JPROC.2015.2494218.